ESTIMATING AND SIMULATING A SIRD MODEL OF COVID-19 FOR MANY
COUNTRIES, STATES, AND CITIES

Jesús Fernández-Villaverde
Charles I. Jones

Estimating and Simulating a SIRD Model of COVID-19 for Many Countries, States, and Cities
Jesús Fernández-Villaverde and Charles I. Jones
NBER Working Paper No. 27128
May 2020, Revised June 2020
JEL No. E0,I0

ABSTRACT

We use data on deaths in New York City, Madrid, Stockholm, and other world cities as well as in various U.S. states and various countries and regions to estimate a standard epidemiological model of COVID-19. We allow for a time-varying contact rate in order to capture behavioral and policy-induced changes associated with social distancing. We simulate the model forward to consider possible futures for various countries, states, and cities, including the potential impact of herd immunity on re-opening. Our current baselinemortality rate (IFR) is assumed to be 1.0% but we recognize there is substantial uncertainty about this number. Our model fits the death data equally well with alternative mortality rates of 0.5% or 1.2%, so this parameter is unidentified in our data. However, its value matters enormously for the extent to which various places can relax social distancing without spurring a resurgence of deaths.

Jesús Fernández-Villaverde
Department of Economics
University of Pennsylvania
The Ronald O. Perelman Center
 for Political Science and Economics
133 South 36th Street Suite 150
Philadelphia, PA 19104
and CEPR
and also NBER
jesusfv@econ.upenn.edu

Charles I. Jones
Graduate School of Business
Stanford University
655 Knight Way
Stanford, CA 94305-4800
and NBER
chad.jones@stanford.edu

A Dashboard of extended results is available at https://web.stanford.edu/~chadj/Covid/Dashboard.html

Change log:

– May 25, 2020: Version 2.0: Drop the "exponential decay" model of β_t. Instead, invert the SIRD model and use death data to recover a β_t and therefore $\mathcal{R}_{0t} = \beta_t/\gamma$ at each date. For simulations of future outcomes, allow for feedback from daily deaths, d_t, to future behavior according to $\mathcal{R}_{0t} = \text{Constant} \cdot d_t^{-\alpha}$ as suggested by Cochrane (2020).

– May 2, 2020: Version 1.0 (NBER working paper). Updated graphs and added a log scale graph of cumulative deaths

– April 28, 2020: Version 0.6: updated based on random testing in New York to a benchmark mortality rate (IFR) of 0.8% and data through April 24. Uses a SIRDC model with 5 states and an "exponential decay" model of β_t.

– April 23, 2020: Version 0.5, first public version, based on a benchmark mortality rate (IFR) of 0.3% and data through April 21.

1. Introduction

We use data on deaths in New York City, Madrid, Stockholm, and other world cities as well as in various U.S. states, countries, and regions around the world to estimate a standard epidemiological model of COVID-19. Relative to existing frameworks, our contributions are

- We do not use data on cases or tests because of differential selection in testing in different cities, states, and countries. Instead we only use data on deaths.

- We invert a standard SIRD epidemiological model and use the daily death series to recover a time-varying $\mathcal{R}_{0t} \equiv \beta_t/\gamma$ to capture changes in behavior and policy that occur at different times and with different intensities in different locations. Relative to our earlier "exponential decay" approach, this formulation has the advantage of being able to capture re-opening effects that may increase contacts.

- We show how simulating our model after a location has reached a peak in the number of daily deaths results in very stable results going forward in time. In contrast, simulations of the future *before* a location reaches its peak are extremely noisy and sensitive to daily shocks.

- For simulations of future outcomes, we allow for feedback from daily deaths, d_t, to future behavior according to $\mathcal{R}_{0t} = \text{Constant} \cdot d_t^{-\alpha}$ as suggested by Cochrane (2020). We estimate α from data for each country. There is tremendous heterogeneity across countries, so this parameter is not well-identified in our data. We estimate an average value of about $\alpha = 0.05$ so that $\mathcal{R}_0$ changes by 5% when daily deaths change by one and use this value in simulations of future outcomes.

- Our models allow us to back out the percent of people who are currently infectious as well as who are ever-infected versus still susceptible and therefore estimate the extent to which herd immunity effects are large. We find moderate effects in New York City, noticeable effects in Italy, Sweden, and Spain, and negligible effects in New York state outside of New York City and in places like California.

We are not epidemiologists, so these results should be interpreted with caution and care. We study a standard model of COVID-19 using common tools in econometrics and then analyze its main quantitative implications in ways that resemble how economists study other dynamic models. Our exercise can help us understand where a simple SIRD model has difficulties fitting observed patterns in the data and points out avenues for improvement while maintaining the virtues of simplicity and parsimony. We plan to update these results regularly on our dashboard, where we also report around 25 pages of graphs for each of around 100 cities, states, and countries.

2. Literature Review

Much of the mathematical study of the spread of infectious diseases start from the classic compartmental models of Kermack and McKendrick (1927) and Kermack and McKendrick (1932). These models divide the population into several different compartments (e.g., susceptible, infective, recovered, deceased, ...) and specify how agents move across the separate compartments over time.[1] The SIRD epidemic model that we analyze in this paper is one of the simplest of these compartmental models. Hethcote (2000) presents a useful overview of this class of models and some of their theoretical

---

[1]Before the contributions of Kermack and McKendrick, William Farr (1807-1883) had observed that epidemics tend to follow a Gaussian curve; however, he never presented a formal mechanism to account for such a pattern.

properties and Morton and Wickwire (1974) shows how to apply optimal control methods to them. Also, Brauer, Castillo-Chavez and Feng (2019) is a recent, comprehensive textbook of the field and Imperial College COVID-19 Response Team (2020) is an example of how these models have been applied to understand the current health crisis by epidemiologists.

The acute economic impact of the current pandemic has generated much interest among economists in exploring compartmental models and how they can be dovetailed into standard economic models and estimated using econometric techniques. (see Stock, 2020, and Avery et al., 2020, for two general surveys of how economists have addressed this topic).

First, economists have argued that many of the parameters controlling the move among compartments are not structural in the sense of Hurwicz (1962), but depend, instead, on individual decisions and policies. For example, the rate of contact that determines the number of new infections is a function of the endogenous labor supply and consumption choices of individuals. Hence, the rate of contact is amenable to be studied with standard decision theory models. See, for instance, Eichenbaum, Rebelo and Trabandt (2020) and Farboodi, Jarosch and Shimer (2020). Also, the recovery and death rates are not just clinical parameters, but can be functions of policy decisions such as expanded emergency hospital capacity or priorities regarding the allocation of scarce ICU resources. Similarly, the case fatality ratio, a key figure to assess the severity of the epidemic, is a complex function of clinical factors (e.g., the severity of a virus) and demographic and selection-into-disease mechanism, which are themselves partly the product of endogenous choices (Korolev, 2020b).[2] Our paper builds on these ideas by allowing the infection rates to be influenced by social distancing and by letting many parameters to vary across countries, states, and cities, which can proxies for demographic and policy heterogeneity.

Second, economists have been concerned with the identification problems of compartmental models. Many of these models are unidentified or weakly identified, with many set of parameters that fit the observed data so far equally well but have considerably different long-run consequences. Atkeson (2020) and Korolev (2020a) document this argument more carefully. Our findings corroborate this result and highlight the

---

[2]More precisely, the case fatality ratio is not the average treatment effect on the treated (ATET), a more explicitly "causal" concept.

need to develop alternative econometric approaches.

Third, some researchers have dropped the use of compartmental models completely. Instead, they have relied on time-series models from the econometric tradition. See, for instance, Linton (2020), Kucinskas (2020), and Liu, Moon and Schorfheide (2020).

Let us close this section by pointing out that economists are pushing the study of compartmental models in a multitude of dimensions. Acemoglu, Chernozhukov, Werning and Whinston (2020), Álvarez, Argente and Lippi (2020), and Chari, Kirpalani and Phelan (2020) characterize the optimal lockdown policy for a planner who wants to control the fatalities of a pandemic while minimizing the output costs of the lockdown. Berger, Herkenhoff and Mongey (2020) analyze the role of testing and case-dependent quarantines. Bethune and Korinek (2020) estimate the infection externalities associated with COVID-19 and find them to be large. Bodenstein, Corsetti and Guerrieri (2020) combine a compartmental model with a multisector dynamic general equilibrium model to capture key characteristics of the U.S. Input-Output Tables. Garriga, Manuelli and Sanghi (2020), Hornstein (2020), and Karin, Bar-On, Milo, Katzir, Mayo, Korem, Dudovich, Yashiv, Zehavi, Davidovich et al. (2020) study a variety of containment policies. Toda (2020), besides also estimating a SIRD model as we do, explores the optimal mitigation policy that controls the timing and intensity of social distancing. More papers are appearing every day.

3. A SIRD Model with Social Distancing

We follow standard notation in the literature. There is a constant population of N people, each of whom may be in one of five states:

$$S_t + I_t + R_t + D_t + C_t = N$$

The states — in temporal order — are

$$
\begin{aligned}
S_t &= \text{Susceptible} \\
I_t &= \text{Infectious} \\
R_t &= \text{Resolving} \\
D_t &= \text{Dead} \\
C_t &= \text{ReCovered}
\end{aligned}
$$

A susceptible person contracts the disease by coming into "adequate" contact with

an infectious person, assumed to occur at rate $\beta_t I_t / N$, where β_t is a time-varying contact rate parameter.

The starting value of β_t, β_0, reflects how the infection would progress if individuals were behaving as they did before any news of the disease had arrived. We think of β_0 as capturing characteristics of the disease, fixed attributes of the region such as density, and basic customs in the region.

Over time, β_t varies depending on how strong is the social distancing and hygienic practices that different locations adopt, either because of policy or simply because of voluntary changes in individual behavior. We will explain below how we recover β_t from the data but, at this moment, we are not imposing any structure on its evolution.[3]

The total number of new infections at a point in time is $\beta_t I_t / N \cdot S_t$. Infectiousness resolves at Poisson rate γ, so the average number of days a person is infectious is $1/\gamma$: e.g., $\gamma = .2 \Rightarrow 5$ days.

After the infectious period is over, a person is in the "Resolving" state, R. A constant fraction, θ, of people exit this state each period, and the case is resolved in one of two ways:

<div align="center">

Death: fraction δ

Recovery: fraction $1 - \delta$

</div>

In earlier versions of this project, we found that it is important to have a model that distinguishes between the infectious and the recovering periods. This distinction was key to matching the data with biologically plausible parameter values when we were putting restrictions on the time path of β_t. In particular, it appears that the infectious period lasts on average about 4 to 5 days while cases take a total of about 2 to 3 weeks or even longer to resolve (Bar-On et al., 2020).[4] If one assumes people are infectious for this entire period, the model has trouble fitting the data.

---

[3]In a previous version of this paper, we imposed that β_t decayed at an exponential rate, as assumed, for example, in Chowell, Viboud, Simonsen and Moghadas (2016). We also tried alternative specifications, including discrete jumps at the time of the introduction of shelter-in-place orders. As we will see below, it turns out that we can dispense from those assumptions and be much more flexible in recovering β_t from observables.

[4]We can also consider the transition to the resolving compartment as reflecting, in part, quarantine measures. While some authors prefer to add a "quarantine" compartment, we did not find we needed it to account for the dynamics of the data.

The laws of motion related to the virus are then given by

$$\Delta S_{t+1} = \underbrace{-\beta_t S_t I_t / N}_{\text{new infections}} \tag{1}$$

$$\Delta I_{t+1} = \underbrace{\beta_t S_t I_t / N}_{\text{new infections}} - \underbrace{\gamma I_t}_{\text{resolving infectious}} \tag{2}$$

$$\Delta R_{t+1} = \underbrace{\gamma I_t}_{\text{resolving infectious}} - \underbrace{\theta R_t}_{\text{cases that resolve}} \tag{3}$$

$$\Delta D_{t+1} = \underbrace{\delta \theta R_t}_{\text{die}} \tag{4}$$

$$\Delta C_{t+1} = \underbrace{(1-\delta)\theta R_t}_{\text{reCovered}} \tag{5}$$

We assume the initial stocks of deaths are set equal to zero. The initial stock of infections and resolving cases, $I(0)$ and $R(0)$, are parameters that we will estimate.

3.1   Basic Properties of a Standard SIRD Model

Here we review the basic properties of this model when $\beta_t = \beta$ and the difference equations are replaced by differential equations (Hethcote, 2000). A convention in epidemiological modeling is to recycle notation and let $\mathcal{R}_0$ denote the basic reproduction number, that is, the expected number of infections generated by the first ill person when $s_0 \equiv S_0/N \approx 1$:

$$\mathcal{R}_0 \quad = \quad \beta \quad \times \quad 1/\gamma$$

# of infections from one sick person	# of lengthy contacts per day	# of days contacts are infectious

More generally, if $\mathcal{R}_0 s_0 > 1$, the disease spreads, otherwise it declines quickly. One can see from this simple equation why $\mathcal{R}_0 > 1$ is so natural: if people are infectious for 5 days and have lengthy contacts with even just two new people per day, for example, then $\mathcal{R}_0 = 10$.

As shown by Hethcote (2000), the initial exponential growth rate of infections is $\beta - \gamma = \gamma(\mathcal{R}_0 - 1)$. Another useful result from these models concerns the long-run number

of people who ever get infected (and therefore the fraction δ of these gives the long-run death rate). As $t \to \infty$, the total fraction of people ever infected, e^*, solves (assuming $s_0 \approx 1$)

$$e^* = -\frac{1}{\mathcal{R}_0} \log(1 - e^*)$$

In other words, with a constant β, the long run number of people ever infected is pinned down by $\mathcal{R}_0$; the parameters γ and θ only affect the timing, holding $\mathcal{R}_0$ constant. The long-run death rate is then δe^*, so this too depends only on $\mathcal{R}_0$ (and δ).

This explains why modeling the changing β associated with social distancing and better hygienic practices is so important. With a constant β, the initial explosion rate of the disease implies a value for β and then all the variables in the differential system are determined at that point. Instead, a changing β permits the initial exponential growth rate of deaths to be different from the long-run properties of the system, which is the point of adopting behavioral changes in society.

4. Recovering β_t and therefore $\mathcal{R}_{0t}$

It turns out that recovering β_t, a latent variable, from the data is straightforward without having to resort to any complex filtering device.

We adopt the following timing convention. D_{t+1} is the stock of people who have died as of the *end* of date $t + 1$, so that $\Delta D_{t+1} \equiv d_{t+1}$ is the number of people who died on date $t + 1$ (daily deaths, in our estimating exercise).

We begin by using equation (4) to solve for various series involving R_{t+1} and its differences in terms of daily deaths:

$$R_t = \frac{1}{\delta\theta}\Delta D_{t+1} = \frac{1}{\delta\theta}d_{t+1} \tag{6}$$

$$\Delta R_{t+1} = \frac{1}{\delta\theta}\left(d_{t+2} - d_{t+1}\right) = \frac{1}{\delta\theta}\Delta d_{t+2} \tag{7}$$

Next, we use (3) and the expressions we just derived for R_{t+1} to solve for I_t and its differences:

$$I_t = \frac{1}{\gamma}\left(\Delta R_{t+1} + \theta R_t\right) \tag{8}$$

$$= \frac{1}{\gamma}\left(\frac{\Delta d_{t+2}}{\delta\theta} + d_{t+1}/\delta\right) \tag{9}$$

$$= \frac{1}{\delta\gamma}\left(\frac{\Delta d_{t+2}}{\theta} + d_{t+1}\right) \tag{10}$$

and applying the difference operator gives:

$$\Delta I_{t+1} = \frac{1}{\delta\gamma}\left[\frac{\Delta d_{t+3} - \Delta d_{t+2}}{\theta} + \Delta d_{t+2}\right] \tag{11}$$

$$= \frac{1}{\delta\gamma}\left(\frac{\Delta\Delta d_{t+3}}{\theta} + \Delta d_{t+2}\right) \tag{12}$$

where $\Delta\Delta d_{t+3} \equiv \Delta d_{t+3} - \Delta d_{t+2}$.

Taking the ratio of (12) to (10) gives:

$$\frac{\Delta I_{t+1}}{I_t} = \frac{\frac{1}{\theta}\Delta\Delta d_{t+3} + \Delta d_{t+2}}{\frac{1}{\theta}\Delta d_{t+2} + d_{t+1}} \tag{13}$$

Now, we can go back to our original SIRD model in equation (2) and rewrite it as

$$\frac{\Delta I_{t+1}}{I_t} = \beta_t\frac{S_t}{N} - \gamma$$

Solve this equation for β_t by using equation (13) above to get

$$\beta_t = \frac{N}{S_t}\left(\gamma + \frac{\Delta I_{t+1}}{I_t}\right)$$

$$= \frac{N}{S_t}\left(\gamma + \frac{\frac{1}{\theta}\Delta\Delta d_{t+3} + \Delta d_{t+2}}{\frac{1}{\theta}\Delta d_{t+2} + d_{t+1}}\right) \tag{14}$$

This is one of the key equations in recovering β_t. Notice, however, that this equation depends on S_t. But since we have an initial condition for S_0, we can use the SIRD model to get the updating equation for ΔS_{t+1} and we will be done. From (1) and using (10) to substitute I_t:

$$\Delta S_{t+1} = -\beta_t S_t\frac{I_t}{N}$$

$$= -\beta_t S_t\frac{1}{\delta\gamma N}\left(\frac{1}{\theta}\Delta d_{t+2} + d_{t+1}\right) \tag{15}$$

or

$$S_{t+1} = S_t \left(1 - \beta_t \frac{1}{\delta\gamma N} \left(\frac{1}{\theta} \Delta d_{t+2} + d_{t+1} \right) \right) \tag{16}$$

Now we only need to collect the last two equations together:

$$\beta_t = \frac{N}{S_t} \left(\gamma + \frac{\frac{1}{\theta}\Delta\Delta d_{t+3} + \Delta d_{t+2}}{\frac{1}{\theta}\Delta d_{t+2} + d_{t+1}} \right) \tag{17}$$

and:

$$S_{t+1} = S_t \left(1 - \beta_t \frac{1}{\delta\gamma N} \left(\frac{1}{\theta} \Delta d_{t+2} + d_{t+1} \right) \right). \tag{18}$$

With these two equations, an observed time series for daily deaths, d_t, and an initial condition $S_0/N \approx 1$, we iterate forward in time and recover β_t and S_{t+1}. Basically, we are using *future* deaths over the subsequent 3 days to tell us about β_t today. While this means our estimates will be three days late (if we have death data for 30 days, we can only solve for β for the first 27 days), we can still generate an informative estimate of β_t.

There are many exercises we can perform with the recovered β_t. We can, for instance, simulate the model forward using the most recent value of β_T and gauge where a region is headed in terms of the infection and current behavior. And we can correlate the β_t with other observables to evaluate the effectiveness of certain government policies such as mandated lock downs.

Note, also, that β_t determines the basic reproduction number, $\mathcal{R}_{0t} = \beta_t \times 1/\gamma$ under the current social distancing and hygienic practices. We should be careful to distinguish this basic reproduction number from the effective reproduction number (i.e., the average number of new infections caused by a single infected individual at time t), which we will denote by R_{et}. The latter considers the fraction of the population that is still susceptible. Since:

$$R_{et} = \mathcal{R}_{0t} \cdot S_t/N,$$

our procedure can also recover the effective reproduction number. This finding is interesting because this effective reproduction number is often reported by researchers due to the easiness with which it can be estimated with standard statistical packages such as `EpiEstim` in `R`.

5. Estimation: Countries and States

The following parameters are assumed to be primarily biological and, therefore, fixed over time and the same in all countries and regions:

- $\gamma = 0.2$: In the continuous time version of this model, the average length of time a person is infectious is $1/\gamma$, so 5 days in our baseline. This choice is consistent with the evidence in Bar-On, Flamholz, Phillips and Milo (2020). We also consider $\gamma = 0.15$ (7 day duration). The $\gamma = 0.2$ fit slightly better in our earlier work with more restrictions on β_t, but it was not particularly well identified.[5]

- $\theta = 0.1$: In the continuous time version of this model, the average length of time it takes for a case to resolve, after the infectious period ends, is $1/\theta$. With $\theta = .1$, this period averages 10 days. Combined with the 5-day infectious period, this implies that the average case takes a total of 15 days to resolve. The implied exponential distribution includes a long tail that can be thought of as capturing the fact that some cases take even longer to resolve.

- $\alpha = 0.05$: For simulations of future outcomes, we allow for feedback from daily deaths per million people, d_t, to future behavior according to $\mathcal{R}_{0t} = \text{Constant} \cdot d_t^{-\alpha}$ as suggested by Cochrane (2020). We estimate α_i from data for each location i. There is tremendous heterogeneity across locations in these estimates, so a common value is not well-identified in our data. We estimate an average value of about $\alpha = 0.05$ so that $\mathcal{R}_{0t}$ changes by 5% when daily deaths change by one. This is the value we use in simulations of future outcomes. More specifically, the mean value of $\hat{\alpha}_i$ in location-specific regressions is 0.066 and the median value is 0.045. However, the standard deviation of $\hat{\alpha}_i$ across locations is a very high 0.15. We report results with both $\alpha = 0$ — i.e., assuming no feedback so that the final value of $\mathcal{R}_{0t}$ that we estimate in the data is assumed to hold in the future — as well as with $\alpha = .05$. The presence of feedback is very clear in our estimation and strikes us as helpful to incorporate, so our baseline results below assume $\alpha = .05$.

---

[5]Note that γ also incorporates choices of individuals and that, therefore, it is not merely pinned down by clinical observations. If an individual experiences symptoms or is suspicious that she might be infectious, hence withdrawing herself from effective contacts with susceptible individuals, we can consider her case has resolved for the purposes of the dynamics of the model, even if she is still under a clinical condition.

- $\delta = 1.0\%$: This parameter is crucial, and it would be great to have a precise estimate of it. Case fatality rates are not helpful, as we do not have a good measure of how many people are infected. Random testing for antibodies to detect how many people have ever been infected is quite informative about this parameter.

The most comprehensive evidence we are aware of comes from a seroepidemiological national survey undertaken by the Spanish Government from April 27 to May 11 to measure the incidence of SARs-CoV-2 in Spain.[6] The survey was large, with 60,983 valid responses from individuals stratified in two stages. Combining the results from this survey with the measured sensitivity and specificity of the test, we conclude that the mortality rate of SARs-CoV-2 in Spain is between 1% and 1.1%. Because many of the early deaths in the epidemic were linked with mismanagement of care at nursing homes in Madrid and Barcelona that could have been avoided, we pick 1% as our benchmark value.

Since mortality rates are affected by the demographic composition of the population (with COVID-19 mortality rates increasing sharply with age), we obtained data on age distributions across countries from the U.N. population division. We decomposed the Spanish mortality rate by age, given the age-specific measured infection incidence rates, and applied those age-mortality rates to the population shares of each country. To control for differences in life expectancy (and hence, for the possibility that the age-specific mortality rate of an 80-year-old individual in a high life-expectancy country is equivalent to the age-specific mortality rate of a 70-year-old individual in a low life-expectancy country), we applied a correction based on the ratio of the life expectancy of each country with respect to Spain's life expectancy.

We found that, for most of the countries in our sample, the estimated mortality rate clusters around 1% (with or without the correction by life expectancy). For example, for the U.S., we found a death rate of 0.76% without correcting for life expectancy and 1.05% correcting by it. Therefore, and parsimoniously, we selected 1% as our baseline parameter values.

Other studies suggest similar values of δ. For instance, on April 23, Governor An-

---

[6]Preliminary report available at https://www.ciencia.gob.es/stfls/MICINN/Ministerio/FICHEROS/ENECOVID_Informe_preliminar_cierre_primera_ronda_13Mayo2020.pdf.

drew Cuomo announced preliminary results suggesting that 21% of New York City residents randomly tested from supermarkets and big-box stores had antibodies for COVID-19. According to New York Department of Health (2020), it takes 3-4 weeks for these antibodies to form, so this suggests that around April 1, 21% of NYC residents were "ever infected." This infection rate is consistent with back-of-the-envelope calculations of death rates of around 0.8%-1%.

Some earlier papers had estimated values of the death rate as low as 0.3%, a value we used in a previous draft of this paper. For instance, Hortasu, Liu and Schwieg (2020) report an IFR of 0.3% using data on travelers from Iceland and some more limited serological studies in Santa Clara County, Los Angeles, and Heinsberg (Germany) also pointed out to death rates between 0.3% and 0.4%. However, some of these studies were criticized for not accounting for the sensibility of testing or were not stratified properly. The current updated evidence suggests that death rates lower than 0.8% are unlikely. Thus, we will report robustness results using death rates of 0.8% and 1.2%.

Data.   Our data are taken from the GitHub repository of Johns Hopkins University CSSE (2020), which reports cumulative death numbers daily for countries, states, counties, and provinces throughout the world. The exception is for the international cities/regions of Lombardy, London, Madrid, Stockholm, and Paris. We obtain data for these locations of the various national vital statistics agencies.

We manipulate this data in three important ways before feeding it into the model. First, on April 15, New York City added more than 3,500 deaths to their counts, increasing the total by more than 43%. We therefore apply this same factor of proportionality (1.4325) to the deaths before April 15 to get a consistent time series for New York City. Second, The Economist (2020) reports that similar adjustments need to be made in other countries. In particular, vital statistics records in countries including Spain, Italy, England, France, and Sweden suggest that "excess deaths" relative to an average over past years exceed deaths officially attributed to COVID-19 by a large margin. We therefore increase deaths in all non-New

York City locations by 33% for all dates.[7] Finally, there are pronounced "weekend effects" in the raw data: there are days, often on the weekend or a holiday, in the middle of the pandemic when a country reports zero deaths, only to make up for this with a spike in deaths in subsequent days. We initially ran the model with this raw data, and it works fine. However, applying a 5-day centered moving average to the data produces more stable results, so we make this final adjustment.

Guide to Graphs. We present our results in several graphs for each country and region. These include cumulative deaths through the latest date, daily deaths (data and simulating forward), and cumulative deaths simulating forward. Data are shown as blue circles or blue bars and simulations are solid lines.

Each graph may have several lines, typically for one of two reasons. In some graphs, we show the simulations from the past seven days. This provides an intuitive assessment of how sensitive the simulations are to one or two recent observations. In other graphs, we show alternatives for baseline, "high," and "low" values of certain parameters.

In these graphs with multiple lines, we use a "rainbow" color scheme. This is easiest to illustrate in the case in which we report simulations from the past seven days. The colors of the rainbow are ordered according to ROYGBIV: red, orange, yellow, green, blue, indigo, violet. We follow this order from oldest to most recent. The only exceptions we make are that "blue" and "indigo" are collapsed into a single color, and the most recent simulation (or baseline value) is always shown in black.

In graphs with three lines, the black line is the baseline value, the red line is a "low" value of the parameter, and the green line is a "high" value, also respecting this rainbow order.

---

[7]Katz and Sanger-Katz (2020) suggest that the excess deaths in New York City could be even larger than the already-adjusted numbers revealed so far: they report 20,900 excess deaths by April 26, compared to 16,673 in the official counts.

Figure 1: New York City: Estimates of $\mathcal{R}_{0t} = \beta_t/\gamma$
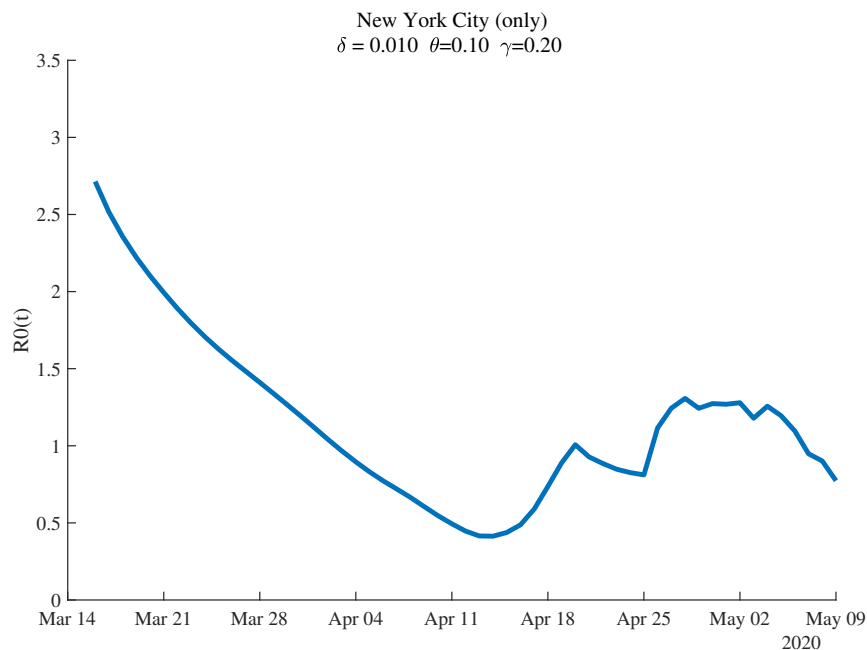
5.1   Baseline Estimation Results

Figure 1 shows the estimates of $\mathcal{R}_{0t} = \beta_t/\gamma$ for New York City. For the baseline parameter values, the estimates suggest that New York City began with $\mathcal{R}_0 = 2.7$, so that each infected person passed the disease to nearly three others at the start. This estimate agrees with other recent findings and its particularly plausible for such a high-density metropolitan area as New York City.[8] Social distancing is estimated to have reduced this value to below 0.5 by mid-April. After that, $\mathcal{R}_{0t}$ seems to fluctuate around 1.0.

It is worth briefly reviewing the data that allows us to recover $\mathcal{R}_{0t}$. As discussed in Section 4, we invert the SIRD model and use the death data to recover a time series for $\mathcal{R}_{0t}$ such that the model fits the death data exactly. In particular, this inversion reveals that $\mathcal{R}_{0t}$ can be recovered from the daily number of deaths (d_{t+1}), the change in daily deaths (Δd_{t+2}), and the change in the change in daily deaths ($\Delta\Delta d_{t+3}$).

---

[8]For instance, Sanche, Lin, Xu, Romero-Severson, Hengartner and Ke (2020) estimate an even higher median $\mathcal{R}_0$ value of 5.7 during the start of the epidemic in Wuhan.

Figure 2: New York City: Daily Deaths and HP Filter

New York City (only): Daily deaths, d
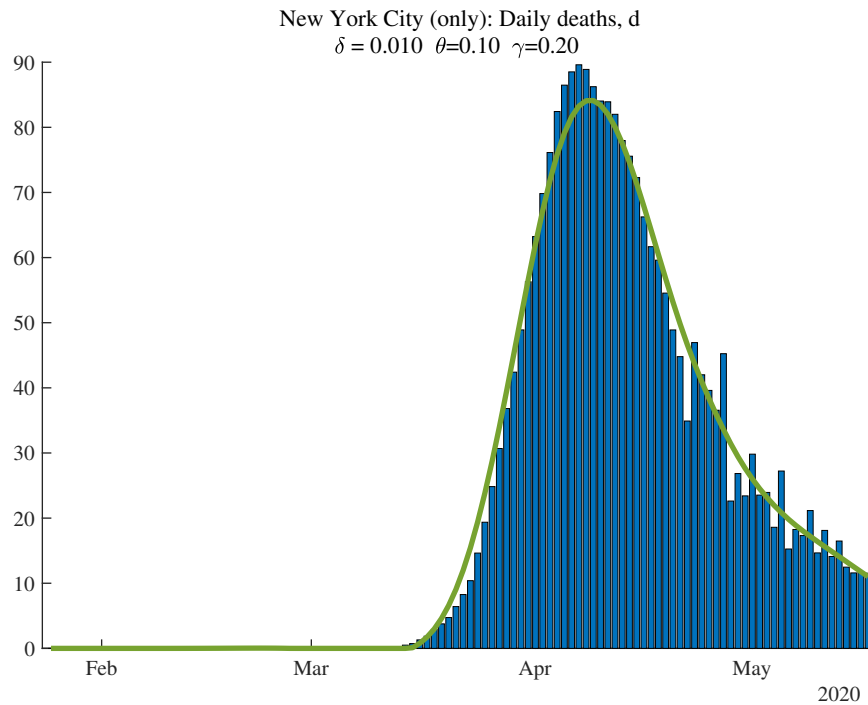$\delta = 0.010 \quad \theta = 0.10 \quad \gamma = 0.20$

Figure 2 shows the data (blue bars) for daily deaths together with an HP filter of that data (with smoothing parameter 200) in green. Figure 3 then shows the change in the HP-smoothed daily deaths, while Figure 4 shows the double difference. It is these HP-filtered data that are used in the construction of $\mathcal{R}_{0t}$ in Figure 1. Because the HP-filter has problems at the end of the sample (e.g. there are fewer observations so noise becomes more important, and double differencing noise reduces precision), the latest estimate of $\mathcal{R}_{0t}$ we have for each location corresponds to May 9, even though our death data runs through May 19: we lose 2 observations for the moving average, 3 observations for the double differencing, and then truncate by an additional 5 days to improve precision.[9]

Our estimation also allows us to recover the fraction of the population that is estimated to be currently infectious at each date. These results are shown for New York City in Figure 5. For our baseline parameter values, this fraction peaks around April 1 at 5.7% of the population. By May 9, it is estimated to have declined

---

[9]These graph of the underlying data are available for every location in our dataset in the extended results on our dashboard.

Figure 3: New York City: Change in Smoothed Daily Deaths

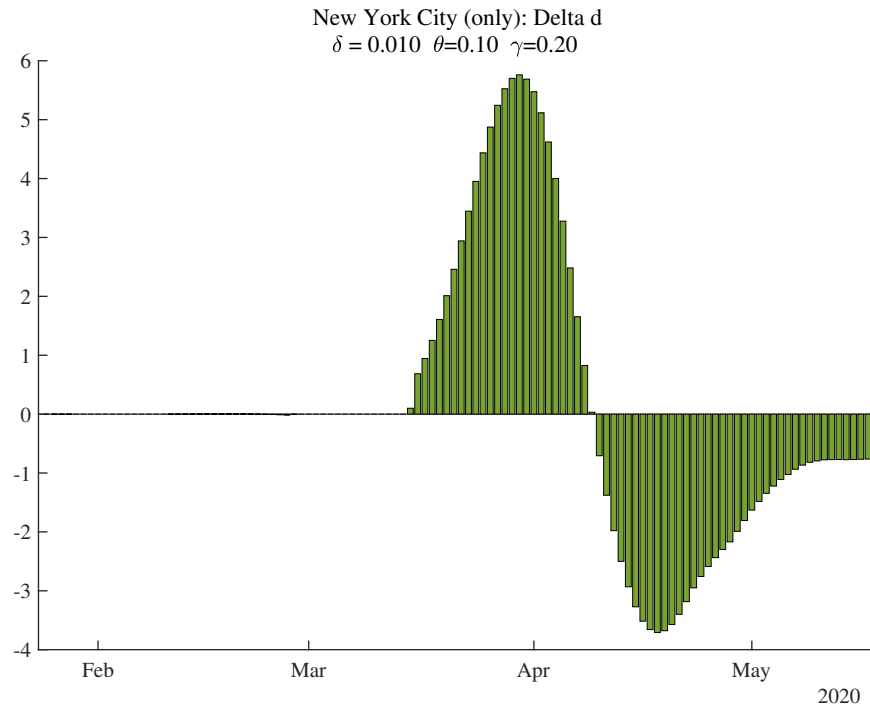New York City (only): Delta d
$\delta = 0.010$ $\theta = 0.10$ $\gamma = 0.20$

Figure 4: New York City: Change in (Change in Smoothed Daily Deaths)

New York City (only): Delta (Delta d)
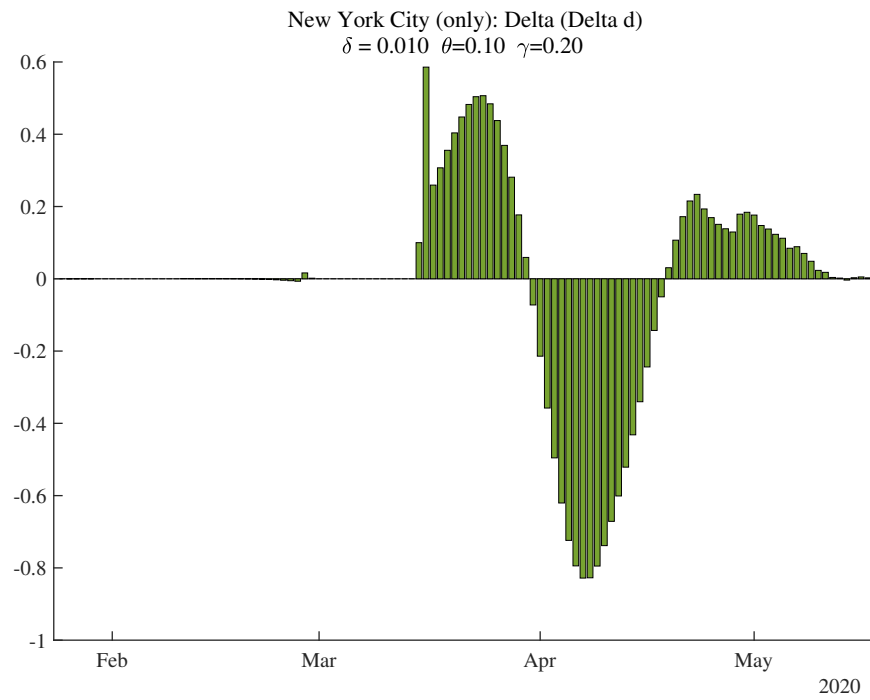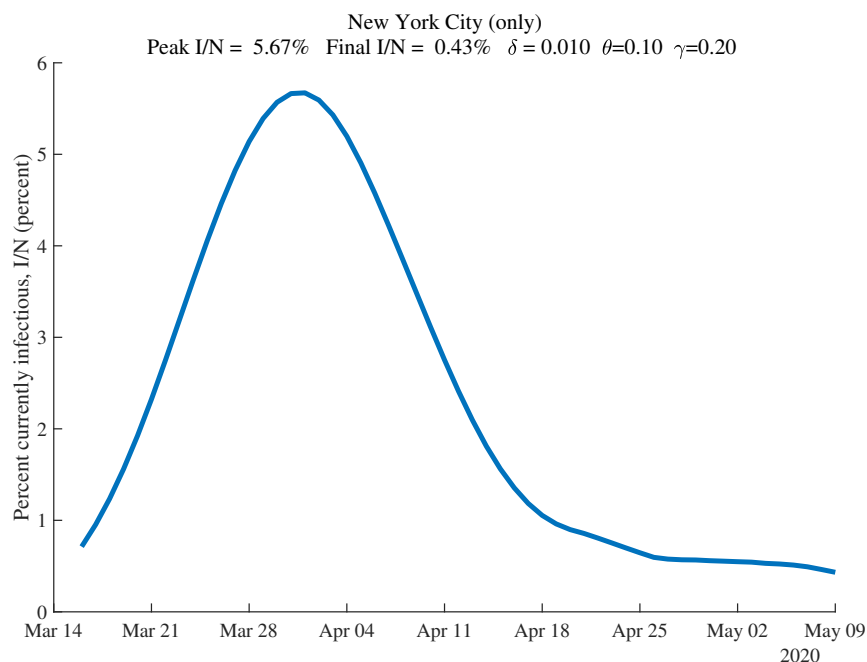$\delta = 0.010$ $\theta = 0.10$ $\gamma = 0.20$

Figure 5: New York City: Percent of the Population Currently Infectious

to only 0.43% of the population.

Figure 6 shows the time path of $\mathcal{R}_{0t}$ for several locations. There is substantial heterogeneity in the starting values, but they all fall and cluster around 1.0 once the pandemic is underway. By the end of the time period, the values of $\mathcal{R}_0$ for Atlanta and Stockholm are noticeably greater than 1.0.

Figure 7 shows the time path of the percent of the population that is currently infectious, I_t/N, for several locations. The waves crest at different times for different locations, and the peak of infectiousness varies as well.

Table 1 summarizes these and other results for a broader set of our locations. The full table, together with ∼25 pages of graphs for each location, are reported on our dashboard. Now is a good time to make a couple of general remarks about our estimation. First, as the number of daily deaths declines at the end of a wave — say for Paris, Madrid, and Hubei in the table — the estimation of $\mathcal{R}_{0t}$ can become difficult and dominated by noise. In the extreme, for example, once total deaths are constant, our procedure gives $\beta_t = 0/0$. One sign of such problems is that "today's" value of $\mathcal{R}_0$ can fall to equal 0.20 — this is a lower bound that we impose

Figure 6: Estimates of $\mathcal{R}_{0t} = \beta_t/\gamma$

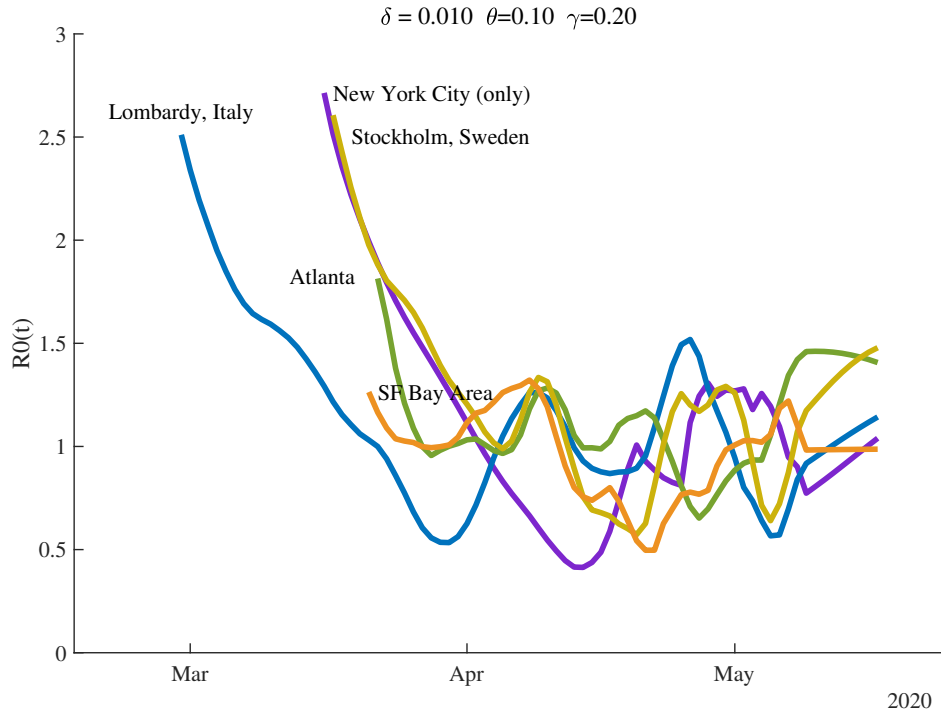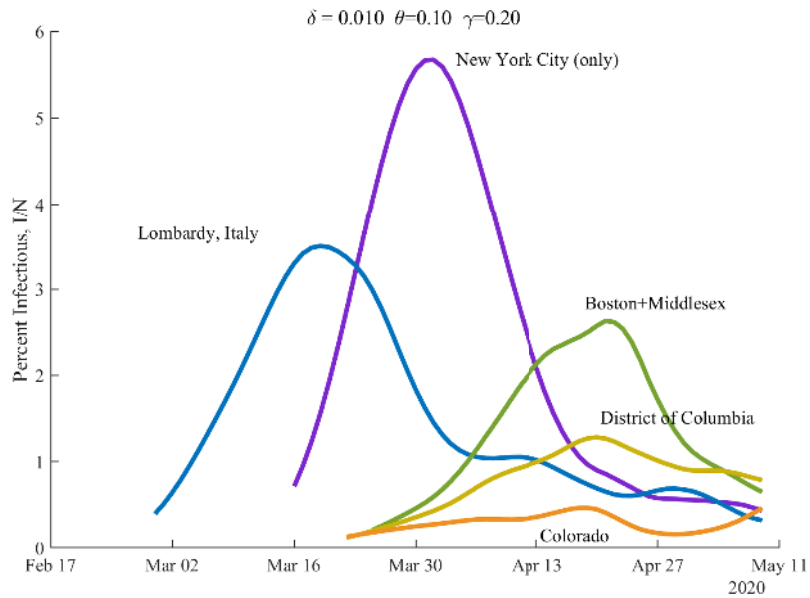$\delta = 0.010 \;\; \theta = 0.10 \;\; \gamma = 0.20$

Figure 7: Percent of the Population Currently Infectious

on the estimation. When a location hits this lower bound, our routine ignores subsequent days of results because the model breaks down. The notation "today" in the table refers to the last day that we have results. Typically it is May 9 when our data runs through May 19, but in some cases it is earlier.

Next, we turn to some general comments about the results. First, notice that the initial values for $\mathcal{R}_0$ range from around 1.5 or lower in places like Minnesota, California, Norway, and Mexico to high values of 2.5 or more in major cities throughout the world. Second, the fraction of the population that is infectious at the peak is greater than 2 percent in the hardest hit areas, but only reaches a maximum of 5.7 percent in New York City. Third, the fraction that is currently infectious today is typically lower. It has fallen below 0.4 percent in New York City (plus), Lombardy, Madrid, Paris, and Detroit but is greater than 0.7 percent in places including New Jersey, Stockholm, Philadelphia, and Chicago. It is even lower — below 0.1 percent — in the SF Bay Area, Washington state, and Germany. Finally, there is of course enormous heterogeneity in cumulative deaths per million people ("Total (pm) Deaths" in the table), both as of today and in the forward simulation for 30 days in the future (t+30).

5.2   Baseline Simulations

Figures 8, 9, and 10 show simulation results for New York City. The black line is the baseline case, with parameter values and estimates reported in the subtitle to the figure. This figure shows results for three values of δ — .01, .008, and .012.

Either higher values of δ such as 1.2% or lower values such as 0.8% can also fit this data — the three lines (black, red, and green) are on top of each other in Figure 8 — so this parameter is not identified.

Next, notice that with these estimates, 26 percent of New York City is estimated to have ever been infected by early May. With $\delta = 1.0\%$, our model implies this number for April 1 was 17%. This compares very well to the recent preliminary announcement by Governor Cuomo that as of April 20, about 21% of New York City residents tested positive for antibodies of COVID-19. Because antibodies only appear 3 to 4 weeks after infection, these antibody tests really tell us what

Table 1: Summary of Results across Locations

	Total (pm) Deaths, t	— $\mathcal{R}_0$ — initial	today	$\mathcal{R}_0 \cdot S/N$ today	% Infectious peak	today	Total (pm) Deaths, t+30
NYC (only)	2482	2.71	0.77	0.57	5.67%	0.43%	2650
NYC (plus)	2116	2.60	0.36	0.28	4.85%	0.35%	2238
Lombardy, Italy	2050	2.51	0.92	0.72	3.50%	0.32%	2236
New York	1451	2.62	0.68	0.57	3.23%	0.36%	1606
Madrid, Spain	1782	2.58	0.20	0.15	3.97%	0.19%	1841
Detroit	1691	2.43	0.50	0.41	2.88%	0.32%	1841
New Jersey	1551	2.61	1.11	0.91	2.44%	0.87%	2137
Stockholm, SWE	1499	2.61	1.17	0.97	2.44%	0.73%	2027
Boston	1198	2.12	0.72	0.62	2.63%	0.65%	1568
Paris, France	1003	2.39	0.20	0.01	1.99%	0.17%	1052
Philadelphia	885	2.46	0.88	0.78	1.68%	0.72%	1291
Michigan	809	2.35	0.69	0.62	1.37%	0.25%	932
Spain	786	2.41	0.53	0.49	1.59%	0.12%	844
Chicago	738	2.17	0.93	0.84	1.10%	1.01%	1144
D.C.	723	1.99	0.94	0.85	1.28%	0.78%	1105
Italy	702	2.22	1.01	0.93	1.07%	0.15%	808
United Kingdom	679	2.37	0.96	0.88	1.16%	0.29%	845
France	567	2.17	1.15	1.07	1.26%	0.17%	682
Sweden	486	2.07	0.90	0.84	0.75%	0.39%	661
Pennsylvania	476	2.06	0.84	0.78	0.89%	0.38%	673
United States	362	2.02	0.91	0.87	0.52%	0.24%	478
NY excl. NYC	264	1.98	1.10	1.06	0.39%	0.39%	456
Miami	275	1.83	0.68	0.66	0.49%	0.23%	354
U.S. excl. NYC	266	1.77	0.95	0.91	0.37%	0.23%	378
Mississippi	239	1.61	0.93	0.89	0.48%	0.26%	369
Los Angeles	192	1.62	1.01	0.98	0.31%	0.20%	294
Minnesota	193	1.54	0.83	0.80	0.36%	0.25%	291
Atlanta	183	1.81	1.46	1.42	0.24%	0.18%	378
Iowa	178	1.44	0.89	0.86	0.35%	0.34%	307
Washington	177	1.56	0.32	0.31	0.26%	0.08%	199
Virginia	170	1.91	0.80	0.77	0.40%	0.16%	230
Germany	127	1.66	0.20	0.18	0.21%	0.04%	135
California	110	1.45	1.04	1.02	0.16%	0.13%	174
Brazil	102	1.26	1.13	1.10	0.28%	0.28%	240
Hubei, China	101	1.40	0.20	0.01	0.23%	0.08%	102
SF Bay Area	77	1.26	0.98	0.97	0.12%	0.04%	97
Mexico	54	1.31	1.12	1.10	0.15%	0.15%	128
Norway	57	1.57	0.20	0.11	0.12%	0.04%	55

Figure 8: New York City: Cumulative Deaths per Million People ($\delta = 1.0\%/0.8\%/1.2\%$)
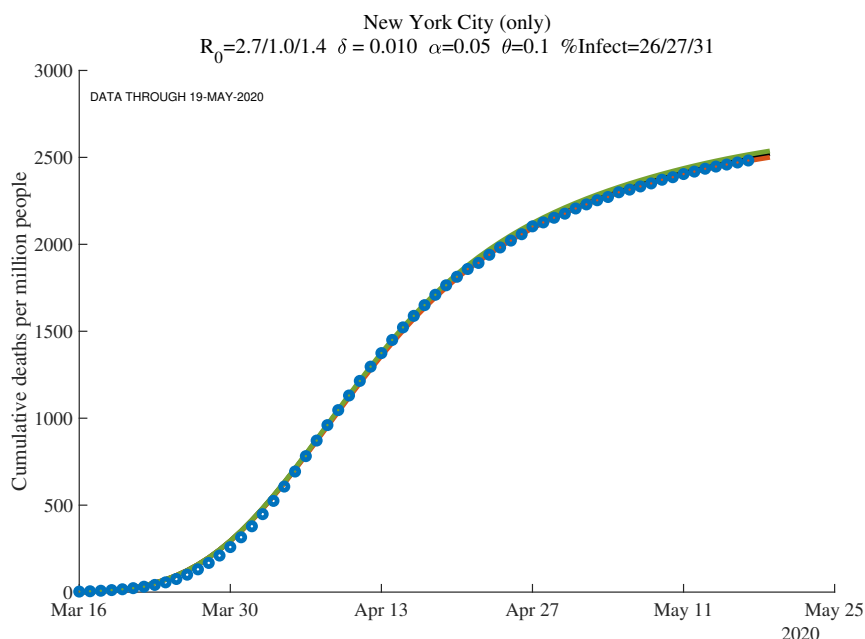
the ever-infected rate was 3 to 4 weeks earlier (New York Department of Health, 2020).

Figure 9 shows the daily number of deaths (per million population) in New York, both in the data and for these same three parameter values. Here it is apparent once again that all three death rates can fit the data equally well.

Figure 10 then shows the cumulative deaths per million, running the simulation forward in time. One might have thought that the different death rates would imply very different futures. However, we re-estimate all parameters when we impose the different death rates, and they all end up producing similar futures in this case. In particular, the simulations imply a death rate by the middle of June of around 2650 people per million. With a population of more than 8 million, this implies approximately 21,000 deaths.

The subtitle lines for these three figures also report the "%Infected" at different dates. These are the percent of people who are estimated to have *ever* been infected with the virus. For New York City, the numbers as of early May are 26 percent, and then in 30 days are estimated to equal 27 percent, with a slightly higher value at the end of our simulation (the third number). We return in Section 7 to

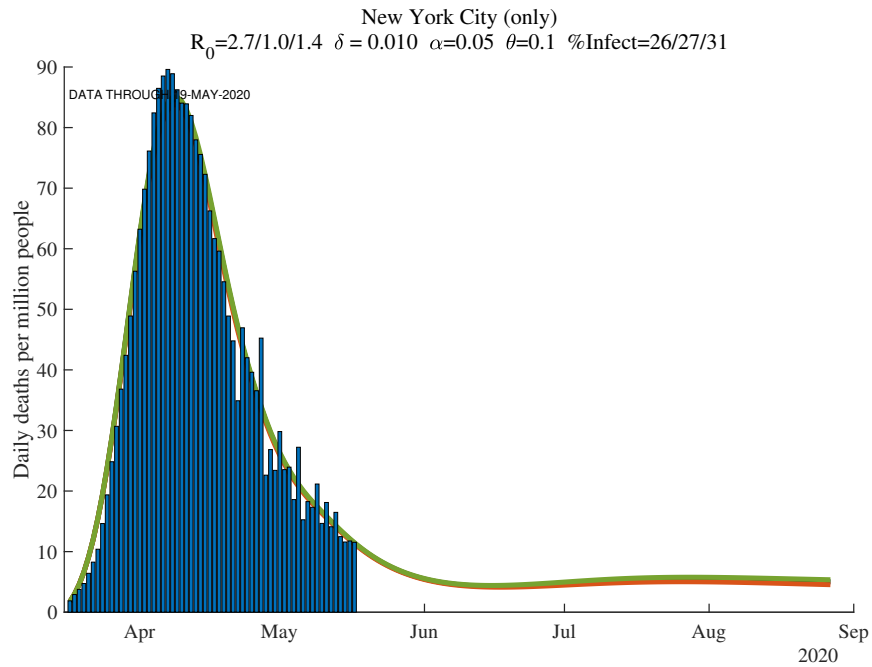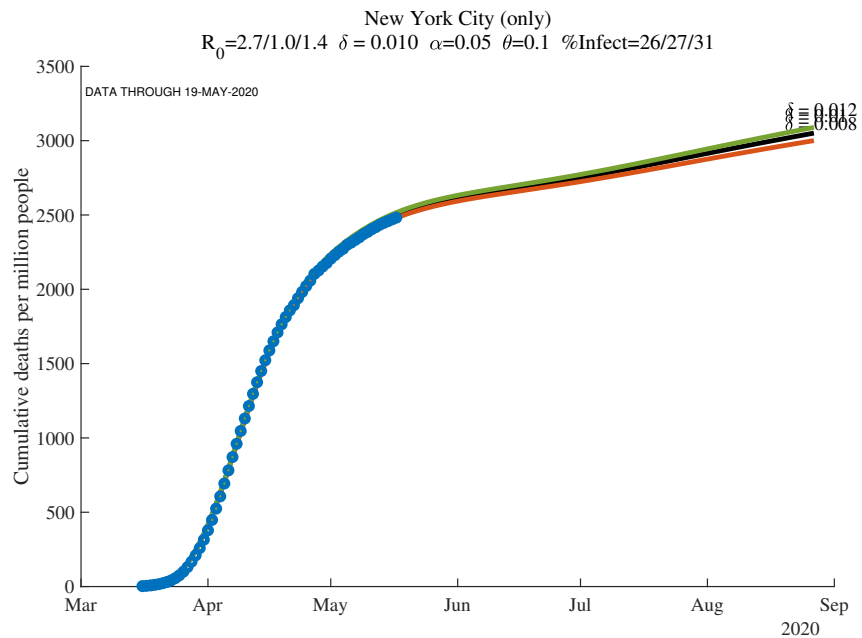Figure 9: New York City: Daily Deaths per Million People ($\delta = 1.0\%/0.8\%/1.2\%$)

New York City (only)
R_0=2.7/1.0/1.4 $\delta = 0.010$ α=0.05 θ=0.1 %Infect=26/27/31

DATA THROUGH 19-MAY-2020

Figure 10: New York City: Cumulative Deaths per Million (Future, $\delta = 1.0\%/0.8\%/1.2\%$)

New York City (only)
R_0=2.7/1.0/1.4 $\delta = 0.010$ α=0.05 θ=0.1 %Infect=26/27/31

DATA THROUGH 19-MAY-2020

$\delta = 0.012$
$\delta = 0.010$
$\delta = 0.008$

the implications of these high infection rates for herd immunity and re-opening.

The next set of graphs show results for Spain together with robustness to different

Figure 11: Spain: Cumulative Deaths per Million People ($\gamma = .2/.1$)
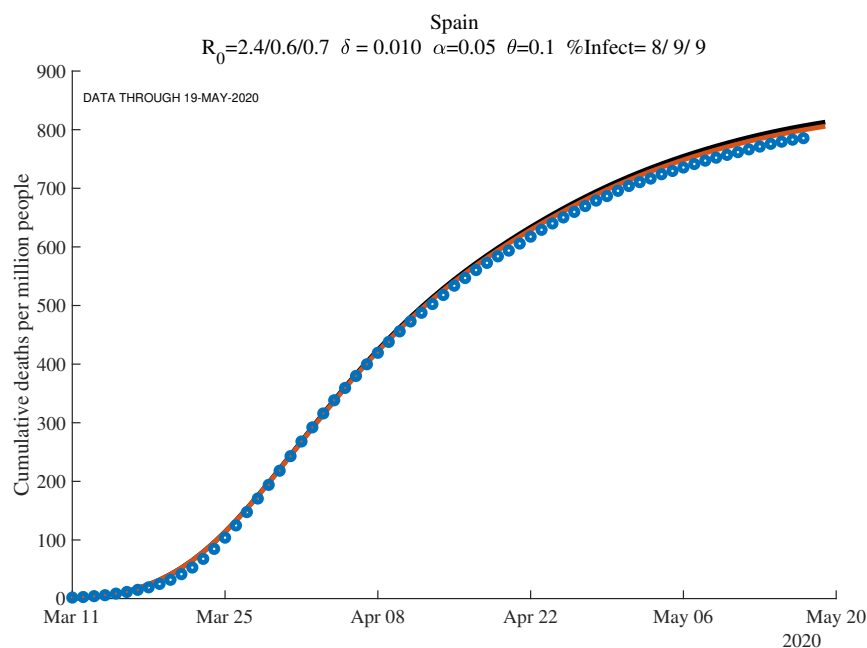
values of γ, the rate at which cases resolve. By construction, our method for recovering a time-varying $\mathcal{R}_{0t}$ means we can fit the data with either parameter value. In our earlier working paper, we found that $\gamma = 0.2$ fit the data better when we had less flexibility in choosing the $\mathcal{R}_0$ values. Moreover, recall $\gamma = 0.2$ corresponds to an average period of infectiousness of 5 days, consistent with the epidemiological literature. Figures 11 and 12 show the results. Spain is estimated to have reduced $\mathcal{R}_0$ from an initial value of 2.4 to 0.6 by early May. Figure 13 suggest that the cumulative number of deaths per million in Spain may level off at around 840.

Next, we show how different values of the recovery-time parameter θ affect our results. Figure 14 shows the daily death numbers for Italy. The fit is good across a range of values for θ, including our benchmark value of $\theta = 0.1$ but also values of 0.07 (in red) and 0.2 (in green).

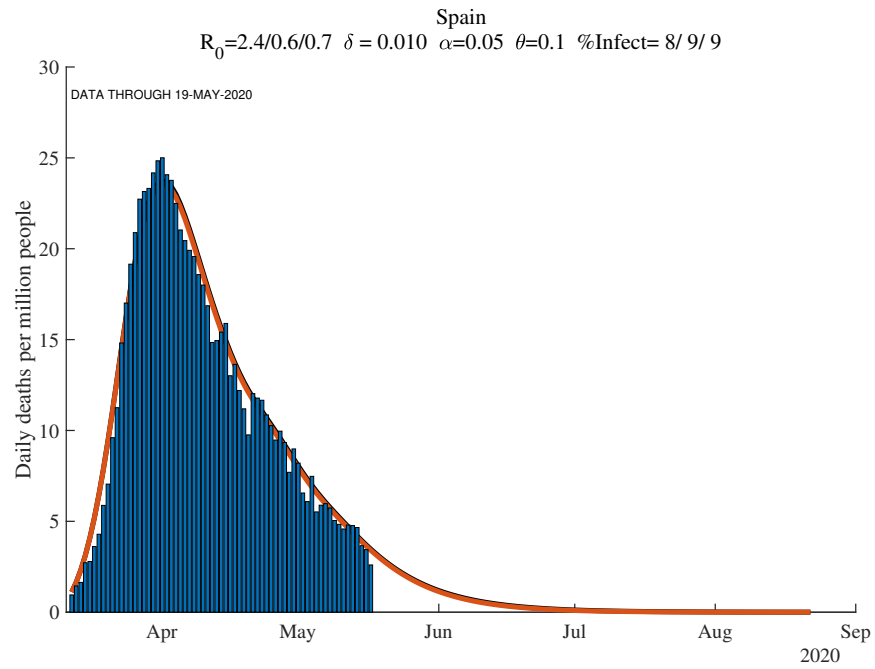Figure 12: Spain: Daily Deaths per Million People ($\gamma = .2/.1$)

Spain
R_0=2.4/0.6/0.7 $\delta = 0.010$ α=0.05 θ=0.1 %Infect= 8/ 9/ 9

Figure 13: Spain: Cumulative Deaths per Million (Future, $\gamma = .2/.1$)

Spain
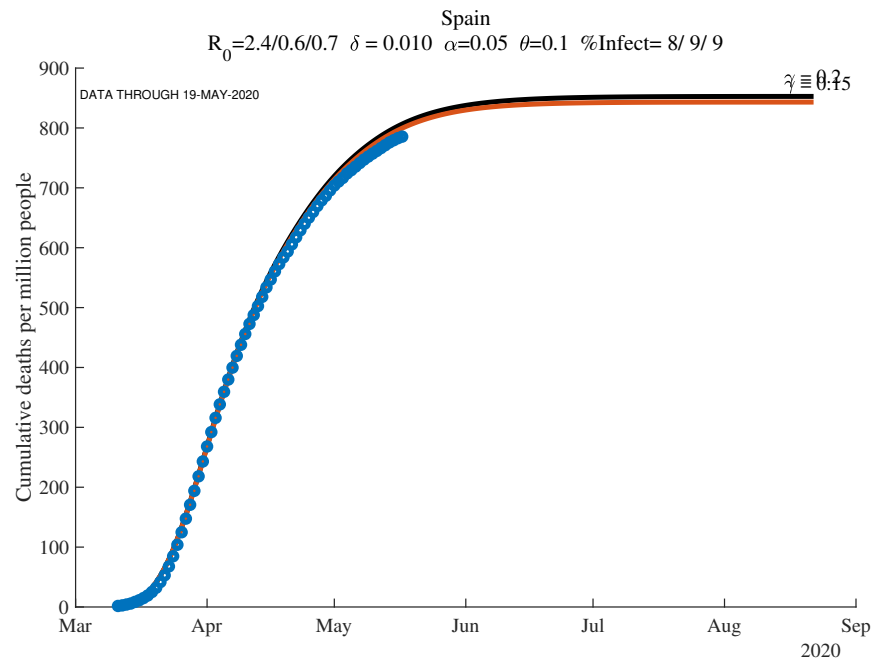R_0=2.4/0.6/0.7 $\delta = 0.010$ α=0.05 θ=0.1 %Infect= 8/ 9/ 9

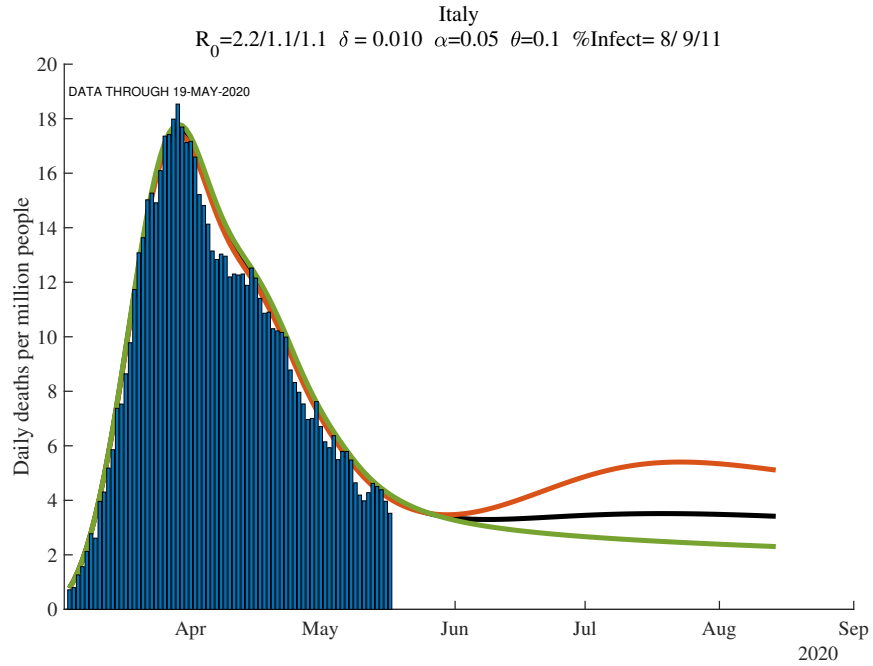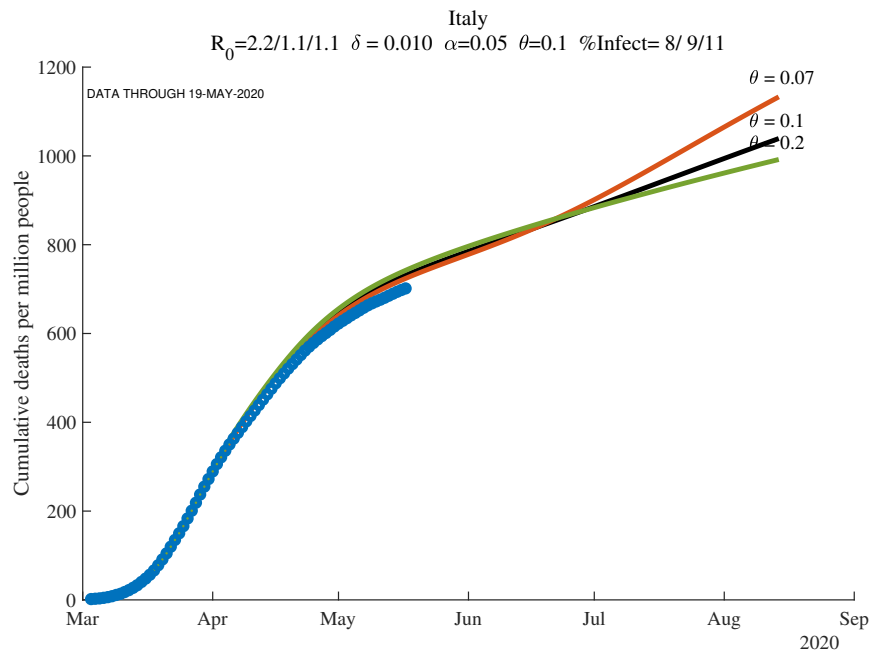Figure 14: Italy: Daily Deaths per Million People ($\theta = .1/.07/.2$)

Figure 15: Italy: Cumulative Deaths per Million (Future, $\theta = .1/.07/.2$)

As we mentioned in the introduction, our online dashboard contains detailed and extended results for around 100 countries, states, and cities. We plan to update it frequently with the latest data:

http://web.stanford.edu/people/chadj/Covid/Dashboard.html.

5.3   Seven Days of Simulations

Our next set of graphs illustrate how the simulations change as we get more data. Two key findings will emerge from these graphs. First, once countries or regions reach the peak and deaths start to decline, the forecasts converge well. Second, however, before that happens, the forecasts are very noisy. This makes sense: we are trying to forecast 30 to 60 days into the future based on 3 to 4 weeks of data using a very nonlinear model.

To begin, we illustrate the first point by showing the simulations for the seven most recent days in Madrid and Lombardy in Figures 16 and 17. Both countries appear to have past their peak deaths and the simulations into the future are relatively similar for the past seven days. Even so, you can see how if deaths come in a little higher than usual, this affects the ending value of $\mathcal{R}_0$ and changes the simulation results for the future. As a reminder, the ordering of the lines follows the colors of the rainbow, with the oldest forecast in red.

New York City.   The next two figures, Figures 18 and 19, show results for New York City now broadly defined to include the surrounding counties of Nassau, Rockland, Suffolk, and Westchester (which we call "New York City (plus)" in the graphs). Like Italy and Spain, New York City is now past its peak, so the forecasts have mostly converged. Nevertheless, when the deaths were flat for a time at the start of May, this suggested that perhaps $\mathcal{R}_0$ had risen somewhat, so the forward simulations were expecting more deaths at that point in time.

California.   The preceding set of graphs show the forecasts converging for Madrid, Lombardy, and New York City. The next set of graphs show the enormous uncertainty that occurs before a region has peaked, in this case in California.

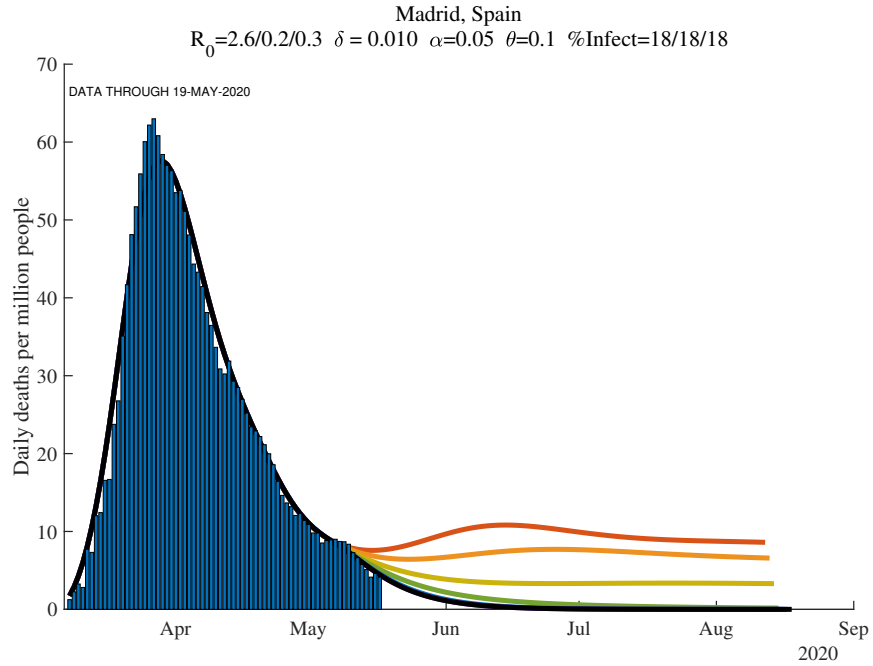Figure 16: Madrid (7 days): Daily Deaths per Million People

Madrid, Spain
R_0=2.6/0.2/0.3 $\delta = 0.010$ α=0.05 θ=0.1 %Infect=18/18/18

Figure 17: Lombardy, Italy (7 days): Daily Deaths per Million People

Lombardy, Italy
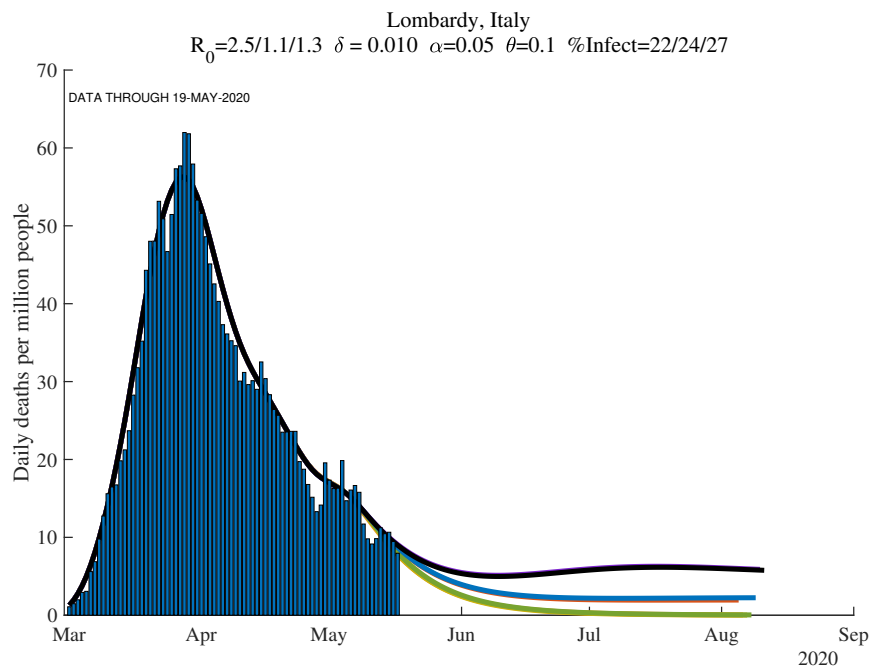R_0=2.5/1.1/1.3 $\delta = 0.010$ α=0.05 θ=0.1 %Infect=22/24/27

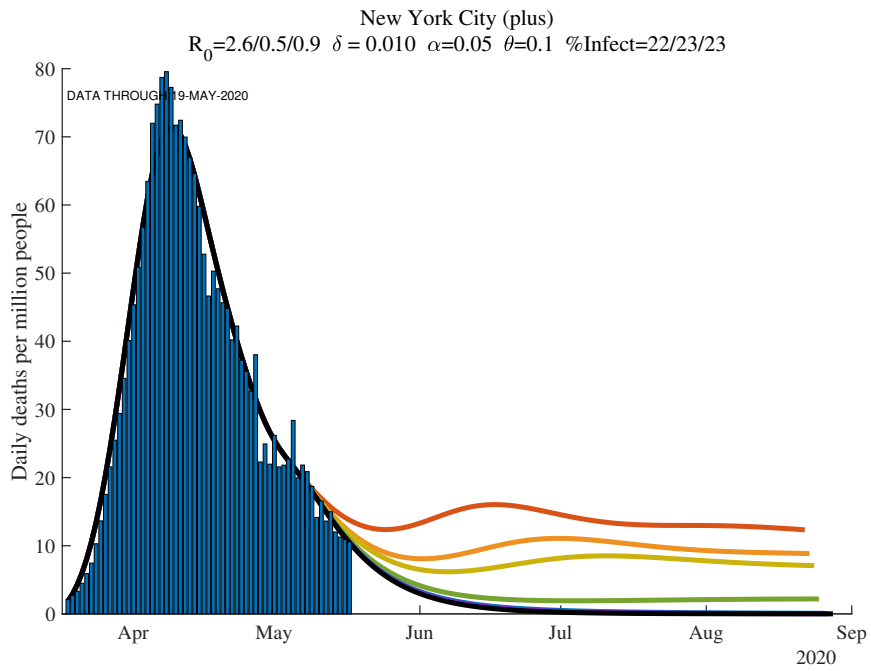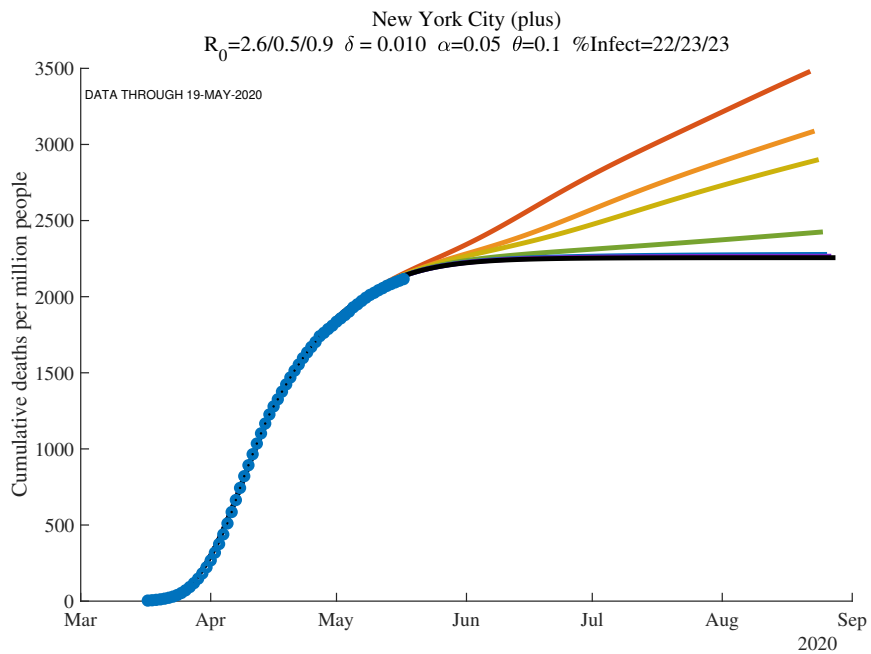Figure 18: New York City (7 days): Daily Deaths per Million People
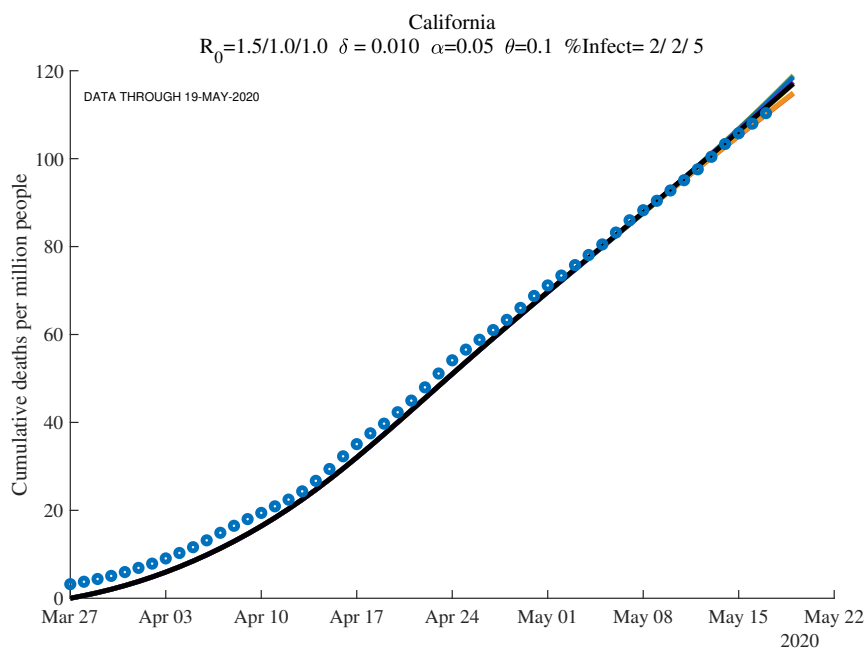

Figure 19: New York City (7 days): Cumulative Deaths per Million (Future)

In Figure 20, the lines change noticeably as each new day provides new data. Notice that the latest parameter values suggest the $\mathcal{R}_0$ fell in California from 1.5

Figure 20: California (7 days): Cumulative Deaths per Million

to 1.0 as a result of social distancing and that only 2 percent of the population of California had ever been infected as of early May. This number is broadly consistent with the recent (but not conclusive) studies of Santa Clara County and Los Angeles, two of the hardest hit places in California, that suggested around 2.5% to 5% of the populations there had been infected (Bendavid et al., 2020).

Figure 21 shows the wild fluctuations in the forecasts of daily deaths in California as new data come in. Notice also that there is no systematic pattern. When deaths come in low, the curves can bend sharply, guessing that the peak has arrived. And when deaths come in high, the curve can unbend and suggest more exponential growth to come.

Now is a useful time to mention the role of the α feedback parameter. In the baseline simulation results in the paper, we assume $\mathcal{R}_{0t} = \text{Constant} \cdot d_t^{-\alpha}$ where $\alpha = 0.05$. This implies that if daily deaths rise, people adjust their behavior to reduce contacts, which reduces $\mathcal{R}_{0t}$. Conversely, if daily deaths fall, people are more likely to go out and interact, which raises $\mathcal{R}_{0t}$.

To see how this affects the results, consider Figure 22, which is based on the same

Figure 21: California (7 days): Daily Deaths per Million People
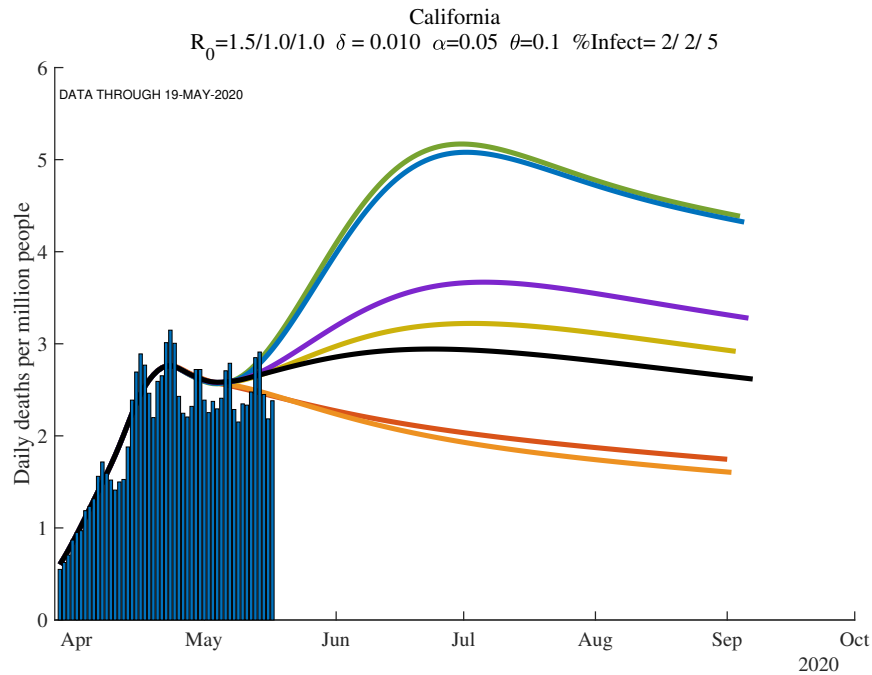
estimation for the past but assumes no feedback between behavior and daily deaths, i.e. by setting $\alpha = 0$. In this case, the swings in daily deaths are must greater with deaths peaking above 20 per day rather than around 5 per day across the different estimates. The key lesson here is that feedback matters tremendously for future outcomes.

Returning to the baseline case of $\alpha = 0.05$, Figure 23 shows the cumulative number of deaths in California going forward. By July, simulation results suggest anywhere from 200 to 300 deaths per million. This compares to a current stock of deaths of around 100 per million.

United Kingdom. A similar illustration of this uncertainty is present in the graphs for the United Kingdom. Figure 24 shows the changing futures as different death numbers come in. $\mathcal{R}_0$ is estimated to have fallen from 2.4 at the start of the pandemic to 1.1 today. The percent ever infected in the U.K. is estimated to be 8 percent as of early May.

The cumulative forecast is then shown in Figure 25. The number of predicted

Figure 22: California (7 days): Daily Deaths per Million People ($\alpha = 0$)

California
R_0=1.5/1.0/1.0 $\delta = 0.010$ α=0.00 θ=0.1 %Infect= 2/ 2/ 5

DATA THROUGH 19-MAY-2020
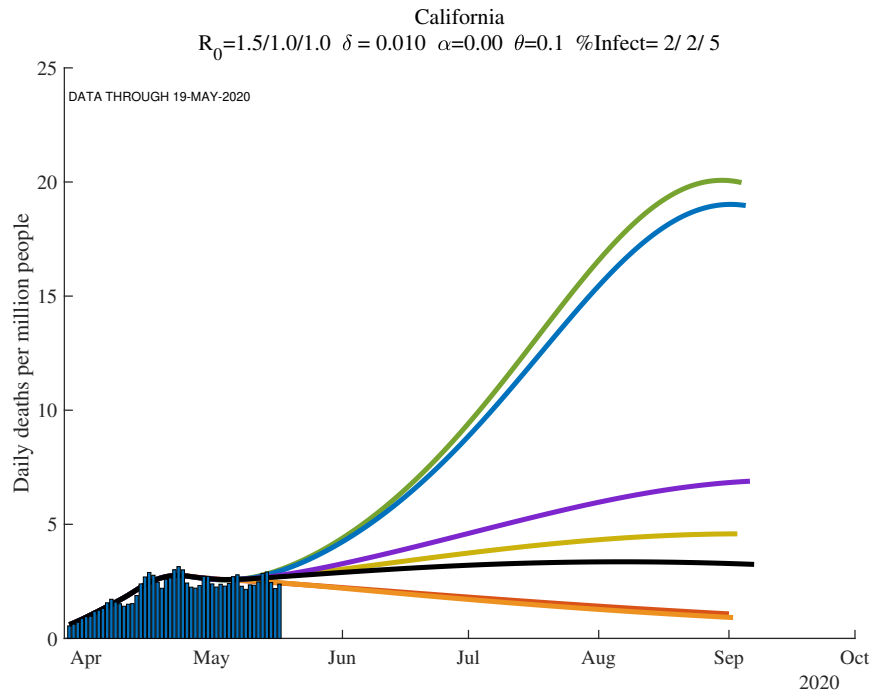
Figure 23: California (7 days): Cumulative Deaths per Million, Log Scale

California
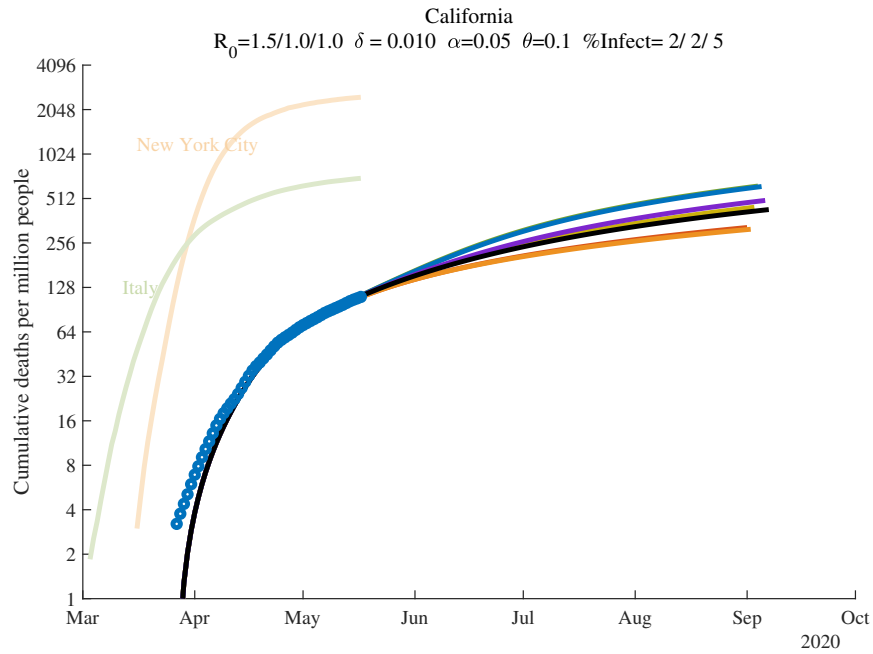R_0=1.5/1.0/1.0 $\delta = 0.010$ α=0.05 θ=0.1 %Infect= 2/ 2/ 5

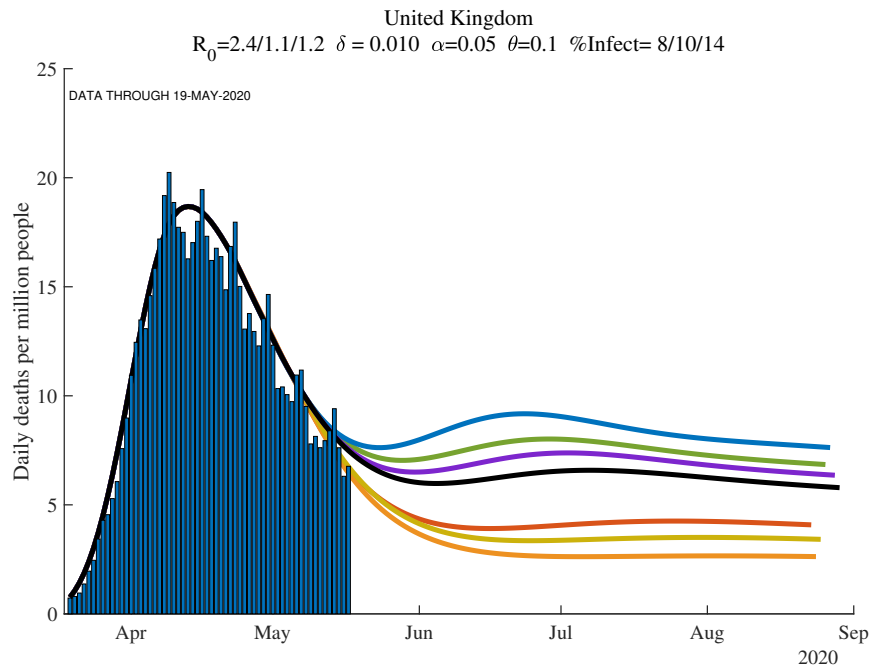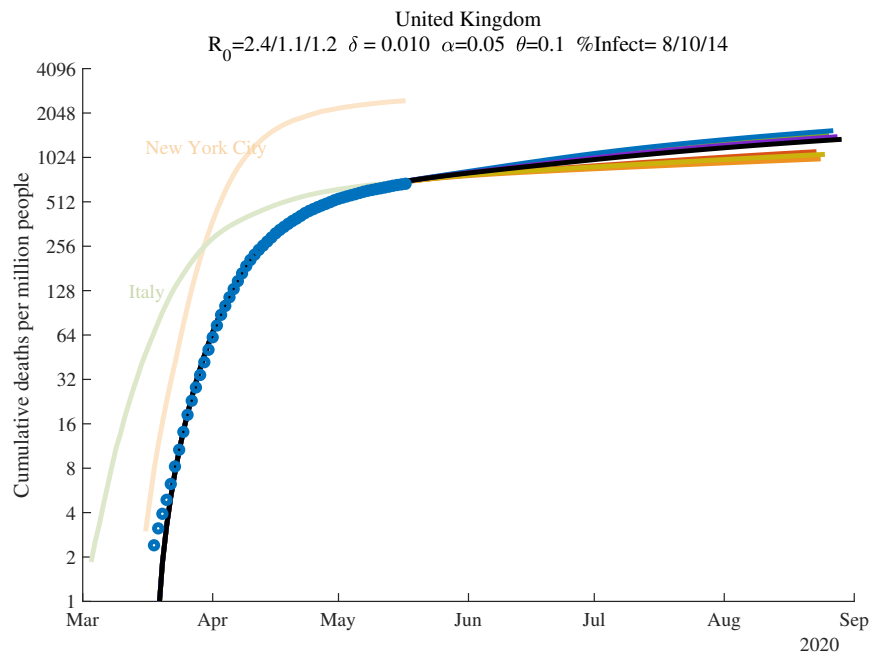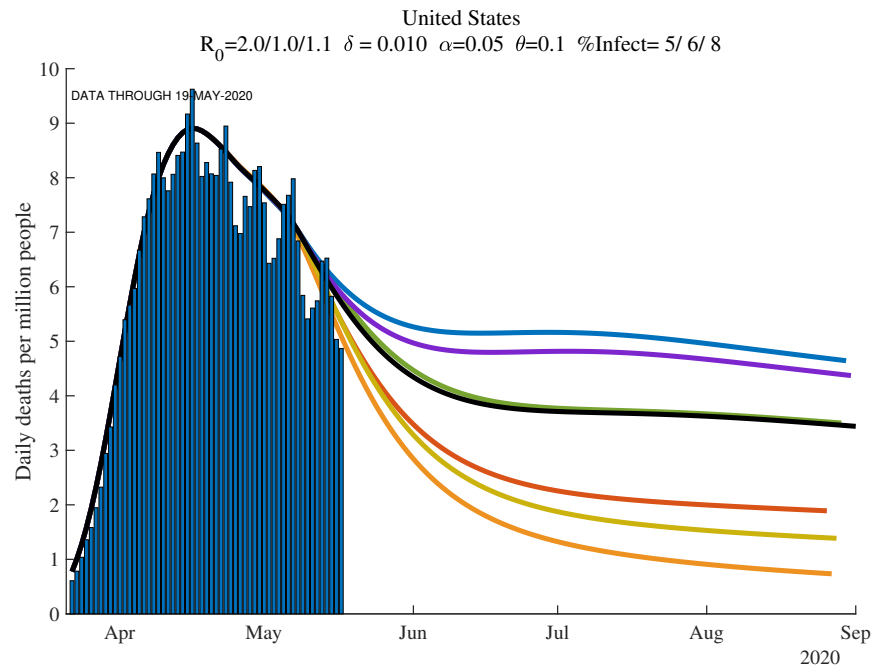Figure 24: United Kingdom (7 days): Daily Deaths per Million People

Figure 25: United Kingdom (7 days): Cumulative Deaths per Million, Log Scale

deaths is high, 850 per million — very similar to Italy.

Figure 26: United States (7 days): Daily Deaths per Million People

United States. Figure 26 shows the daily death numbers for the United States as a country. Despite our smoothing, there are still some "day of the week" effects in these data, which results in some variation in the forward simulations.

The cumulative forecast is then shown in Figure 27. The number of predicted deaths is relatively high, with the lowest number as of July 1 being around 400 per million. Notice that even this low-end death rate implies 120,000 deaths for the United States by mid summer, and the number is projected to go even higher. By September, the latest estimate implies more than 700 deaths per million, or more than 230,000 total deaths.

Boston. To see another example where this convergence has not yet occurred, consider Boston, shown in Figures 28 through 29. The outcome over the next month or two in Massachusetts is still quite uncertain.

Sweden. Sweden is another very interesting case. As has been noted, Sweden's public policy approach has differed from that in many other countries. In par-

Figure 27: United States (7 days): Cumulative Deaths per Million, Log Scale

United States
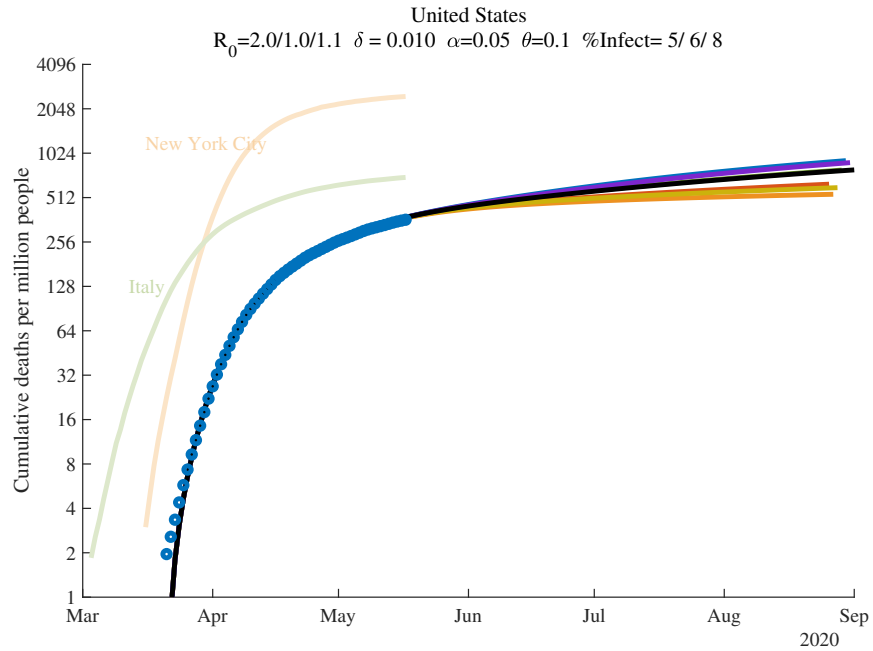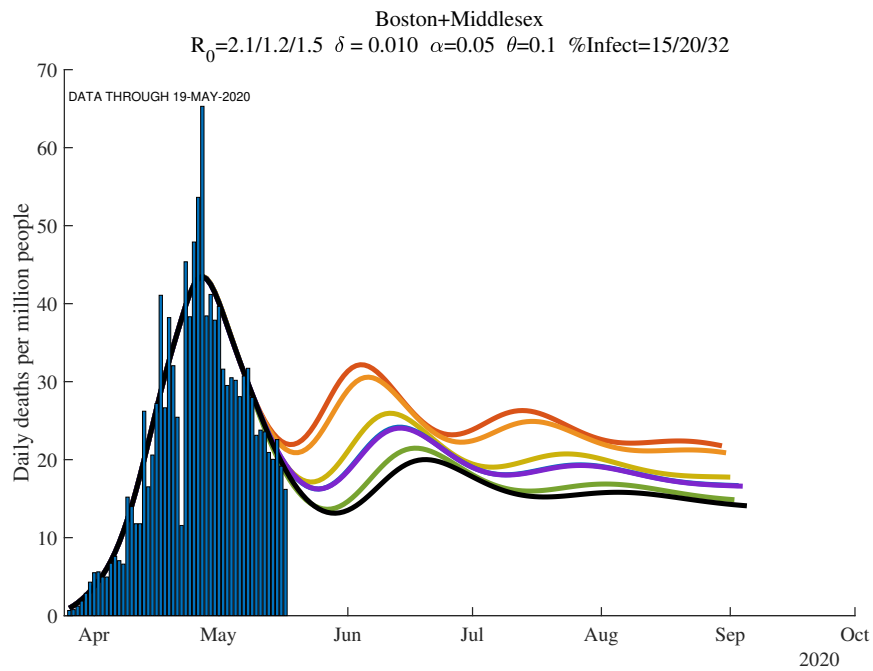$R_0=2.0/1.0/1.1$ $\delta = 0.010$ $\alpha=0.05$ $\theta=0.1$ %Infect= 5/ 6/ 8

Figure 28: Boston (7 days): Daily Deaths per Million People

Boston+Middlesex
$R_0=2.1/1.2/1.5$ $\delta = 0.010$ $\alpha=0.05$ $\theta=0.1$ %Infect=15/20/32

ticular, one stylized view is that Sweden is trying to split its population into two groups based on their different propensities to die if infected. A "high death rate" group, for example the elderly and younger people who might be particularly susceptible because of existing medical problems, could be encouraged to stay home. The remaining "low death rate" group could be allowed to work, go to school, and more generally remain involved in society. In this way, herd immunity could potentially be achieved with a limited number of deaths. At this point, the high risk group could be allowed to gradually reintegrate, possibly with masks and other social distancing protocols in place.

Figures 30 and 31 show the results so far in Sweden. Two things stand out. First, the percent of the overall population estimated to be infected is relatively low, at 6 percent. This low number assumes a common death rate of 1.0%, but later on in the paper in Table 2, we show that even with a death rate of 0.5%, only 12 percent of Sweden's population is estimated to be infected. Second, the number of cumulative deaths is not especially low, having already reached more than 480 deaths per million people and projected to go even higher. This of course does not mean that the stylized policy presented in the previous paragraph is not worth trying and potentially valuable. In fact, a model of this kind of possibility is studied by Acemoglu, Chernozhukov, Werning and Whinston (2020) and policies that exploit heterogeneity in the extent to which different populations may die from the virus can lead to better outcomes in their setup. Perhaps Sweden did not succeed in implementing such a policy or perhaps it doesn't work after all for some reason. More work will be needed on this question.

Other countries. The appendix and the dashboard contain additional graphs for other countries and regions. The patterns, uncertainties, and biases we have highlighted above are apparent in these graphs as well. These graphs will be updated frequently.

Figure 29: Boston (7 days): Cumulative Deaths per Million, Log Scale

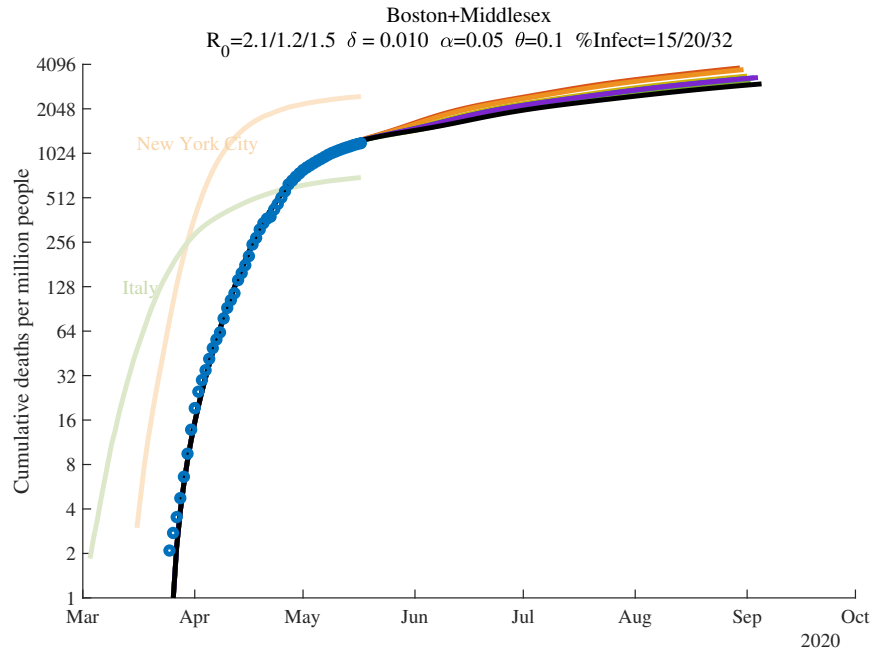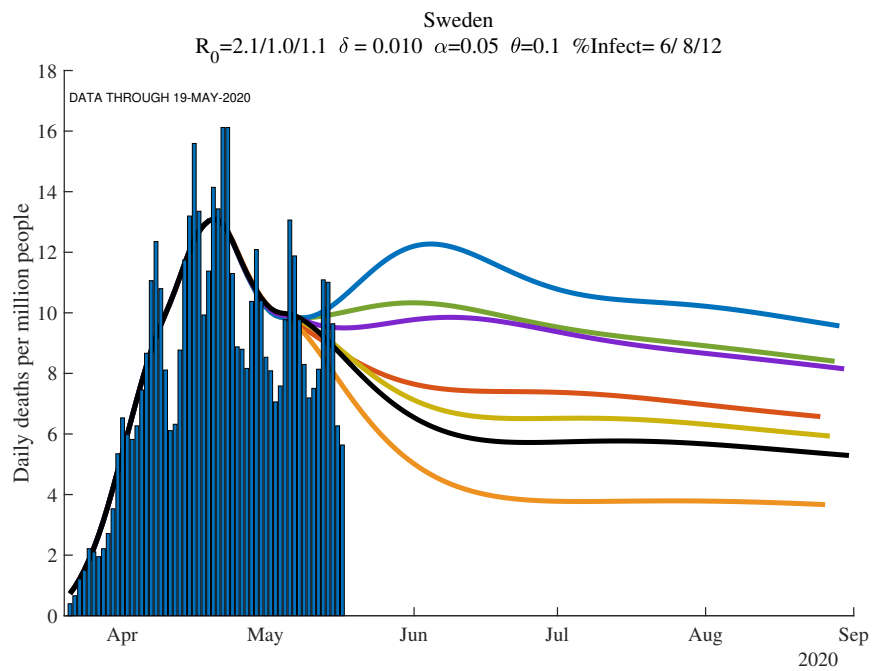Boston+Middlesex
R_0=2.1/1.2/1.5 δ = 0.010 α=0.05 θ=0.1 %Infect=15/20/32

Figure 30: Sweden (7 days): Daily Deaths per Million People

Sweden
R_0=2.1/1.0/1.1 δ = 0.010 α=0.05 θ=0.1 %Infect= 6/ 8/12

6. Problems with Geographic Aggregation

A point that is important to appreciate is that aggregating up from the city or county to the state and to the national level can be misleading. SIRD is a nonlinear model, so the results at the state level are not the same as the average of the results at the county level.

This point is easy to illustrate using data from New York. We report results for several different geographic regions. "New York City (plus)" includes New York City plus the four surrounding counties of Nassau, Rockland, Suffolk, and Westchester, with a total population of about 12 million. New York state is self explanatory and has a population of about 20 million. And "New York excluding NYC" is the difference between these other two: New York state excluding the NYC (plus) area, with a population of about 8 million.

Now compare the results for these three regions, shown in Figures 32 through 34. The results in New York state as a whole are driven entirely by New York City. For example, imagine (counterfactually) that there were no deaths outside of New York City. In this hypothetical case, deaths per million for New York state would look exactly like deaths per million for New York City, except scaled down by a factor of 12/20. Because of the lower deaths per million, the model would behave slightly differently — New York state would be slower to achieve herd immunity for example. And yet New York outside of New York City could look very different. In fact, as the deaths in New York City decline, a potential rise in deaths outside of New York City could cause the state death numbers to exhibit a flattening or even a second peak.

Another version of this same kind of geographic aggregation bias seems likely to occur for the United States itself (look back at Figure 26. To see this, imagine 50 states that sequentially pass through the peak of daily deaths. The U.S. national number can be driven by New York (City!) for the first several weeks, then by New Jersey and Michigan, and then by Massachusetts and Pennsylvania. The U.S. graph may show a rise and then a very flat profile of deaths that persists for a long time before declining, as new regions within the country suffer through their peaks sequentially.

Figure 31: Sweden (7 days): Cumulative Deaths per Million, Log Scale

Sweden
R_0=2.1/1.0/1.1 δ = 0.010 α=0.05 θ=0.1 %Infect= 6/ 8/12
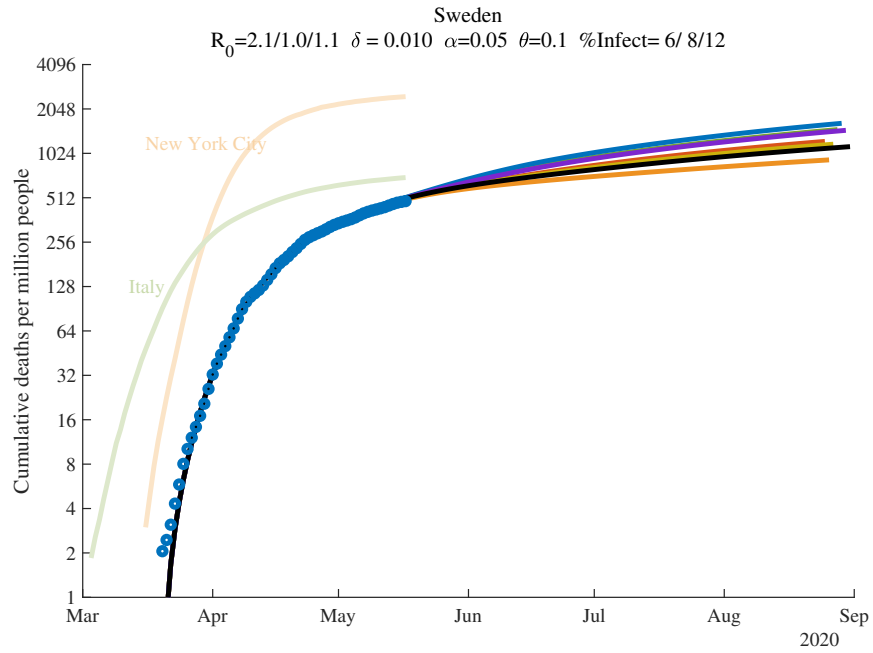
Figure 32: New York City (plus): Daily Deaths per Million People

New York City (plus)
R_0=2.6/0.5/0.9 δ = 0.010 α=0.05 θ=0.1 %Infect=22/23/23
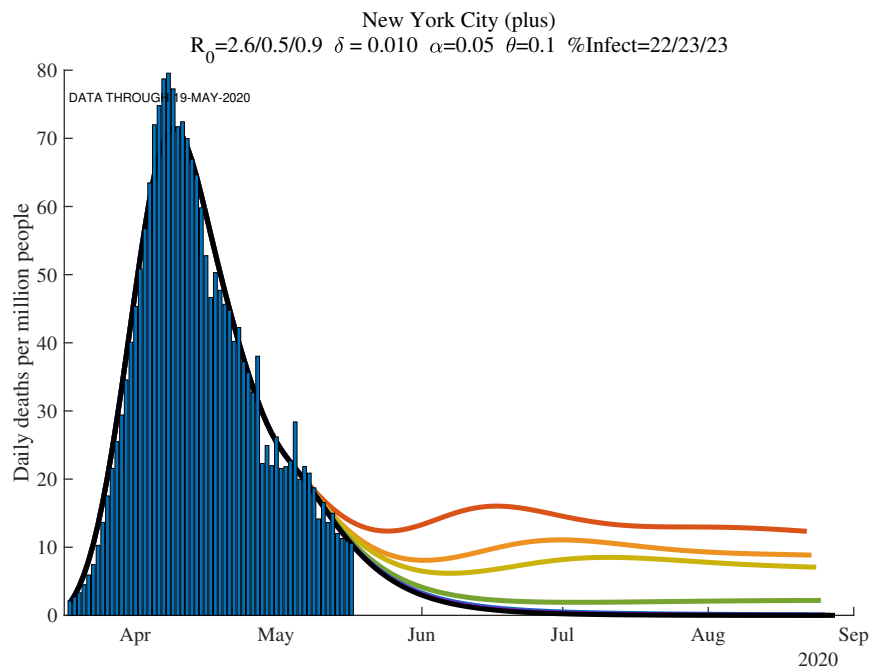
Figure 33: New York State: Daily Deaths per Million People

New York
R_0=2.6/0.9/1.2 δ = 0.010 α=0.05 θ=0.1 %Infect=16/17/18

DATA THROUGH 19-MAY-2020
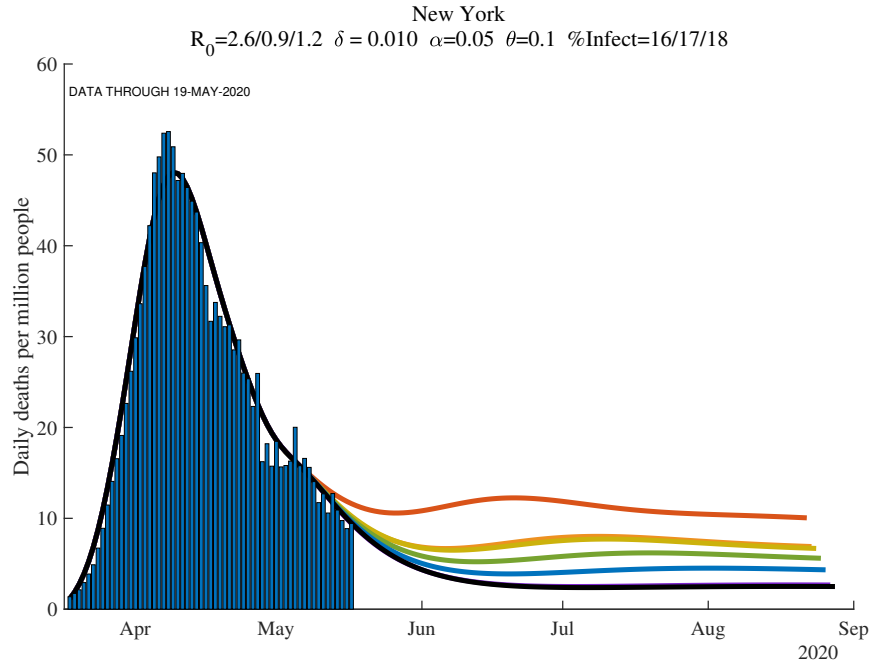
Figure 34: New York excluding NYC: Daily Deaths per Million People

New York excluding NYC
R_0=2.0/1.0/1.1 δ = 0.010 α=0.05 θ=0.1 %Infect= 4/ 6/12

DATA THROUGH 19-MAY-2020
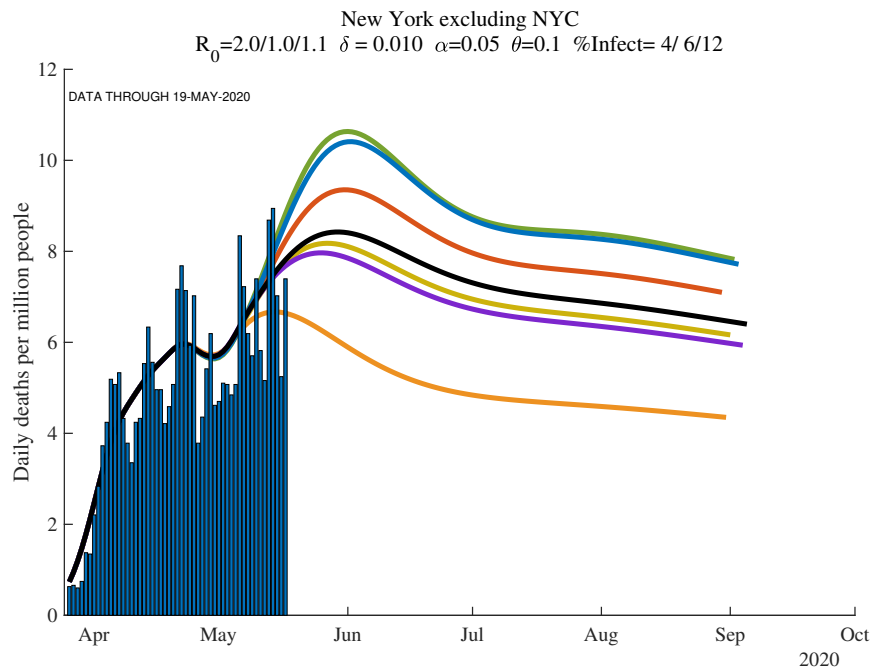
7. Herd Immunity and Re-Opening the Economy

An important question at this stage of the pandemic is how we go about re-opening the economy. The estimation we've conducted has something helpful to contribute on this point.

First, Table 2 reports the estimated fraction of the population that has ever been infected as of May 9 for different countries and regions. Values for three different values of δ are also reported, with the baseline case of $\delta = 1.0\%$ in the center column. Two key things stand out in the table. First, consider the baseline. As we discussed above, we estimate that 26% of New Yorker City have ever been infected.

In contrast, only 4 percent of people in New York state outside of New York City and only 2 percent of Californians have ever been infected. There is enormous heterogeneity in ever-infected rates. Where do these numbers come from? In our model, the fraction δ of those infected eventually die, with the timing determined by γ and θ, but essentially suggesting that deaths today reflect infections from 15 days earlier. With an assumed death rate of $\delta = 1.0\%$, for each death, there are approximately 100 other people who have been infected. The large differences in the number of deaths per million in New York versus California then translate into these differences in infection rates. Interestingly, rates in Norway and South Korea are similarly very low, while ever-infected rates in Italy, Spain, and France are estimated to be around 6 to 8 percent.

The second point is that these numbers are — in an obvious way — very sensitive to the assumed value of δ. If you double the death rate, you (roughly) halve the ever-infected rate. If you halve the death rate, you (roughly) double the infected rate. And as we discuss in more detail next, in thinking about herd immunity and re-opening the economy, knowing the fraction ever-infected is crucial, at least under the important assumption that antibodies give rise to immunity for an extended period of time.

Notice that there is an important complementarity here. We would like the death rate to be low, not just because it means that fewer people die, but also because it means that lots of people will already have been infected. For example, if the

Table 2: Why Random Testing Would Be So Valuable

| | — Percent Ever Infected (today) — | | |
	$\delta = 0.5\%$	$\delta = 1.0\%$	$\delta = 1.2\%$
New York City (only)	51	26	22
New York City (plus)	44	22	19
Lombardy, Italy	43	22	19
New York	31	16	13
Madrid, Spain	36	18	15
Detroit	36	18	15
New Jersey	37	19	16
Stockholm, Sweden	36	18	15
Connecticut	33	17	14
Boston+Middlesex	29	15	12
Massachusetts	29	15	12
Paris, France	21	11	9
Philadelphia	23	12	10
Michigan	18	9	8
Spain	17	8	7
Chicago	21	11	9
District of Columbia	20	10	8
Italy	15	8	7
United Kingdom	16	8	7
France	13	6	5
Illinois	13	7	6
Sweden	12	6	5
Pennsylvania	12	6	5
United States	9	5	4
New York excluding NYC	8	4	3
Miami	7	3	3
U.S. excluding NYC	7	4	3
Ecuador	6	3	3
Los Angeles	5	3	2
Minnesota	5	3	2
Atlanta	5	3	2
Iowa	6	3	2
Florida	3	2	1
Germany	3	1	1
California	3	2	1
Brazil	4	2	2
Mexico	2	1	1
Norway	1	1	0

true death rate is 5 in 1000 rather than 10 in 1000, it means that 51 percent of New Yorkers have already been infected and the herd immunity effects would be very strong. In this sense, the finding that only 21 percent of New York City as ever infected as of April 1 was doubly bad news: it pushes up the death rate and means we are far from herd immunity, even in the place with the largest number of infections.

As Atkeson (2020), Stock (2020), and others have emphasized, random testing would be extremely helpful in identifying which of these cases is relevant. Moreover, the table suggests that if we are going to do 1000 random tests, you would much rather do them in New York City than in California. So few people are likely infected in California that it would be very hard to distinguish statistically between the different death rates, whereas even 1000 random tests would be very informative in New York City.

7.1   How far can we relax social distancing?

This brings us to the next reason why knowing the percent ever infected would be so useful. The complement of this number is the percent of the population that is still susceptible to the virus. Call this fraction $s(t) \equiv S(t)/N$ (or better might be $S(t)/(N - D(t))$ but $D(t)$ is so low that it makes no difference).[10]

Recall from the basic SIR model that the virus will die out as long as

$$\mathcal{R}_0(t)s(t) < 1$$

That is, if $\mathcal{R}_{0t} \equiv \beta_t/\gamma$ is smaller than $1/s(t)$. The term $s(t)$ is the herd immunity term. The fewer people who are susceptible and the more people who are recovered and hence immune, the less our random interactions result in infections. In particular, we can relax social distancing — increase β_t and $\mathcal{R}_{0t}$ — to the critical value such that $\mathcal{R}_{0t}s(t)$ is just below one. That would mean that today's infected people infect fewer than one person on average, so the herd immunity keeps the virus from re-surging.

---

[10]Notice, however, that our very stylized SIRD model is silent about how you map concrete policy decisions (i.e., should we or not open non-essential businesses) into changes in $\mathcal{R}_{0t}$.

Table 3: Using Percent Susceptible to Estimate Herd Immunity, $\delta = 1.0\%$

	$\mathcal{R}_0$	$\mathcal{R}_{0t}$	Percent Susceptible t+30	$\mathcal{R}_0$(t+30) with no outbreak	Percent way back to normal
New York City (only)	2.7	0.8	73.5	1.4	30.3
New York City (plus)	2.6	0.4	77.5	1.3	41.5
Lombardy, Italy	2.5	0.9	77.5	1.3	23.4
New York	2.6	0.7	83.8	1.2	26.4
Madrid, Spain	2.6	0.2	81.5	1.2	43.2
Detroit	2.4	0.5	81.6	1.2	37.6
New Jersey	2.6	1.1	78.3	1.3	11.4
Stockholm, Sweden	2.6	1.2	78.3	1.3	7.2
Boston+Middlesex	2.1	0.7	84.9	1.2	32.9
Massachusetts	2.1	1.0	83.3	1.2	21.3
Paris, France	2.4	0.2	89.4	1.1	42.0
Philadelphia	2.5	0.9	87.2	1.1	17.0
Michigan	2.4	0.7	90.6	1.1	25.0
Spain	2.4	0.5	91.5	1.1	29.8
Chicago	2.2	0.9	87.0	1.1	18.0
District of Columbia	2.0	0.9	87.9	1.1	19.0
Italy	2.2	1.0	91.5	1.1	6.8
United Kingdom	2.4	1.0	91.0	1.1	10.0
France	2.2	1.1	91.9	1.1	-6.0
Illinois	2.0	0.9	91.2	1.1	15.3
Sweden	2.1	0.9	92.7	1.1	15.2
Pennsylvania	2.1	0.8	93.0	1.1	19.5
United States	2.0	0.9	94.7	1.1	13.1
New York excluding NYC	2.0	1.1	92.8	1.1	-2.3
Miami	1.8	0.7	96.3	1.0	31.0
U.S. excluding NYC	1.8	0.9	95.6	1.0	11.8
Ecuador	1.5	0.8	95.7	1.0	30.8
Los Angeles	1.6	1.0	96.2	1.0	5.4
Minnesota	1.5	0.8	96.7	1.0	28.7
Atlanta	1.8	1.5	86.2	1.2	-84.9
Iowa	1.4	0.9	96.1	1.0	27.2
Washington	1.6	0.3	98.0	1.0	56.3
Florida	1.6	0.9	98.0	1.0	15.3
Germany	1.7	0.2	98.6	1.0	55.8
California	1.5	1.0	97.5	1.0	-3.4
Brazil	1.3	1.1	95.0	1.1	-54.7
SF Bay Area	1.3	1.0	98.8	1.0	10.3
Mexico	1.3	1.1	97.3	1.0	-45.8
Norway	1.6	0.2	99.4	1.0	58.9

Table 3 shows these calculations for one month from now $(t + 30)$ given the baseline estimates from the model. For example, from the middle column, it is estimated that in one month's time, 78 percent of New York City (plus surrounding counties) will still be susceptible. This means we could relax social distancing to the point where $\mathcal{R}_0$ would rise to $1/0.78 = 1.3$. This compares to the current estimate for New York City of 0.4 and the initial estimate of 2.6. In other words, a month from now, in this simulation (which may not adequately capture the real world!), New York City could move 41% ([1.3-0.4]/[2.6-0.4]) of the way back to normal and see no re-surgence of the virus.

The rest of the state of New York, in contrast, is estimated to still have 93% of the population susceptible a month from now. So outside of the city, New York needs to maintain its $\mathcal{R}_0$ at 1.1 — also its current level — to keep the virus from spreading. New York City and the rest of New York state need different policies if the fraction of the population that remains susceptible is as different as these estimates imply.

Places with current values of $\mathcal{R}_0 < 1$ can relax somewhat and still keep the virus in check. But the basic news from this table is that with a death rate of 1%, there is very little herd immunity that has been accumulated and our scope for relaxing social distancing is limited.[11]

On the other hand, if somehow this 1% death rate is overstated and the true death rate is only 0.5%, the picture changes. The herd immunity effects for this case are shown in Table 4. In this case, the greater New York City area has only about 56% of its population susceptible because ever-infected rates are much higher. New York City could move 57 percent of the way back to normal, raising $\mathcal{R}_0$ to 1.8, and still not see a resurgence of the virus. Other places would also have more scope to relax social distancing, at least somewhat.

This is why random testing in several places with a relatively high deaths per million is so important: it will help us learn whether the numbers in Table 3 or 4 are more relevant.

---

[11]Notice, also, that these computations assume that individuals stay within their territories, and do not move among them, mixing infection rates across areas.

Table 4: Herd Immunity with a Much Lower Death Rate, $\delta = 0.5\%$

	$\mathcal{R}_0$	$\mathcal{R}_{0t}$	Percent Susceptible t+30	$\mathcal{R}_0(t+30)$ with no outbreak	Percent way back to normal
New York City (only)	2.7	1.6	46.6	2.1	51.1
New York City (plus)	2.6	0.7	56.1	1.8	56.6
Lombardy, Italy	2.5	1.5	54.4	1.8	30.6
New York	2.6	1.0	67.5	1.5	28.1
Madrid, Spain	2.6	0.3	64.1	1.6	55.9
Detroit	2.4	1.0	63.5	1.6	41.3
New Jersey	2.6	1.9	49.1	2.0	20.1
Stockholm, Sweden	2.6	1.8	52.1	1.9	11.6
Boston+Middlesex	2.1	1.4	61.8	1.6	33.7
Massachusetts	2.1	1.5	58.9	1.7	37.2
Paris, France	2.4	0.3	79.3	1.3	46.5
Philadelphia	2.5	1.3	66.9	1.5	13.2
Michigan	2.4	0.9	80.8	1.2	22.1
Spain	2.4	0.6	83.3	1.2	31.5
Chicago	2.2	1.1	71.3	1.4	30.1
District of Columbia	2.0	1.2	72.0	1.4	26.7
Italy	2.2	1.2	82.7	1.2	4.6
United Kingdom	2.4	1.2	80.8	1.2	7.2
France	2.2	1.2	84.3	1.2	-5.7
Illinois	2.0	1.0	81.4	1.2	21.7
Sweden	2.1	1.0	84.6	1.2	16.1
Pennsylvania	2.1	1.1	83.4	1.2	12.5
United States	2.0	1.0	89.0	1.1	11.8
New York excluding NYC	2.0	1.1	87.7	1.1	6.7
Miami	1.8	0.8	92.4	1.1	29.8
U.S. excluding NYC	1.8	1.0	90.8	1.1	11.2
Ecuador	1.5	0.9	91.2	1.1	36.1
Los Angeles	1.6	1.0	92.4	1.1	6.7
Minnesota	1.5	0.9	93.1	1.1	28.5
Atlanta	1.8	1.4	87.5	1.1	-77.7
Iowa	1.4	0.9	92.2	1.1	33.9
Washington	1.6	0.3	96.0	1.0	57.4
Florida	1.6	1.0	96.0	1.0	14.1
Germany	1.7	0.2	97.3	1.0	56.5
California	1.5	1.0	95.3	1.0	0.7
Brazil	1.3	1.1	92.5	1.1	4.4
SF Bay Area	1.3	1.0	97.7	1.0	11.0
Mexico	1.3	1.1	95.7	1.0	-17.4
Norway	1.6	0.2	98.9	1.0	58.9

7.2   What happens if we re-open the economy?

We now show simulations of what happens if we relax social distancing and in-
crease the value of $\mathcal{R}_0$ (i.e., β). The next set of graphs assume that more generous
policies are adopted one month from "today," (which varies by country), i.e., on
something like June 9. Four simulation results are shown in each graph:

– The black line assumes the $\mathcal{R}_0$ from early May remains in place forever.

– The red line assumes that $\mathcal{R}_0$ rises slightly to $1/s(t)$, i.e., to the level that
would just keep the virus from exploding based on the current number of
susceptible people (as of early May again).

– The green line assumes we increase $\mathcal{R}_0$ by 25% back toward normal, i.e., by
25% of the way back from the May 9 estimate toward the initial level of $\mathcal{R}_0$.

– Finally, the purple line is similar except we increase $\mathcal{R}_0$ by to 50% of the way
back to normal.

For these simulations, we assume that the new value of $\mathcal{R}_0$ remains in place for-
ever. In practice, of course, one imagines that if deaths started to rise significantly,
mitigation policies would be re-adopted.

For comparison, these graphs also show — in the light brown bars — the daily
deaths per million in New York City. This is helpful in judging how severe a resur-
gence of the virus might be in different scenarios. For example, if Spain were
to move 50 percent of the way back to normal (the purple line), the predicted
resurgence would be much more severe than New York City experienced. Even
with a 25 percent return to normal, the rise in deaths would be comparable to
New York City, albeit with a lag into the late summer.

Finally, note that the SIRD model has "momentum." Even if an area has reached
the threshold $\mathcal{R}_0(t)s(t) < 1$, we will continue accumulating infections and deaths
before the epidemic dies out fully. The number of these "overshoot" infections
and deaths will depend on the number of infectious individuals when we reach
$\mathcal{R}_0(t)s(t) < 1$. This observation is not a minor point. In a conventional SIRD
model where $\mathcal{R}_0(t)$ gives you herd immunity at 60% of the population, if we reach
$s(t) = 0.4$ too fast, we can end up with over 90% of the population ever infected,

Figure 35: Spain: Re-opening
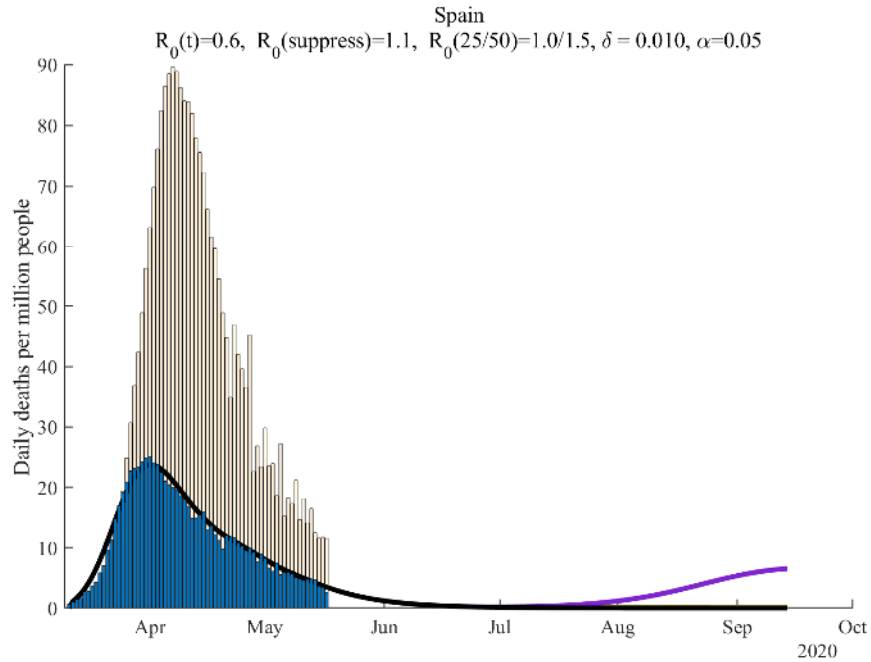
that is, with an extra 30% of infections over those required to achieve herd immunity.

This means that we want to reach the threshold $\mathcal{R}_0(t)s(t) < 1$ or stay around it with very few infectious individuals to minimize "overshoot" infections. While setting up and solving an optimal control problem of the COVID-19 epidemic in the tradition of Morton and Wickwire (1974) to get to such an objective is beyond the scope of our paper, our empirical results can help to calibrate re-opening scenarios such as those quantitatively explored in Baqaee, Farhi, Mina and Stock (2020).

Figure 36: Italy: Re-opening
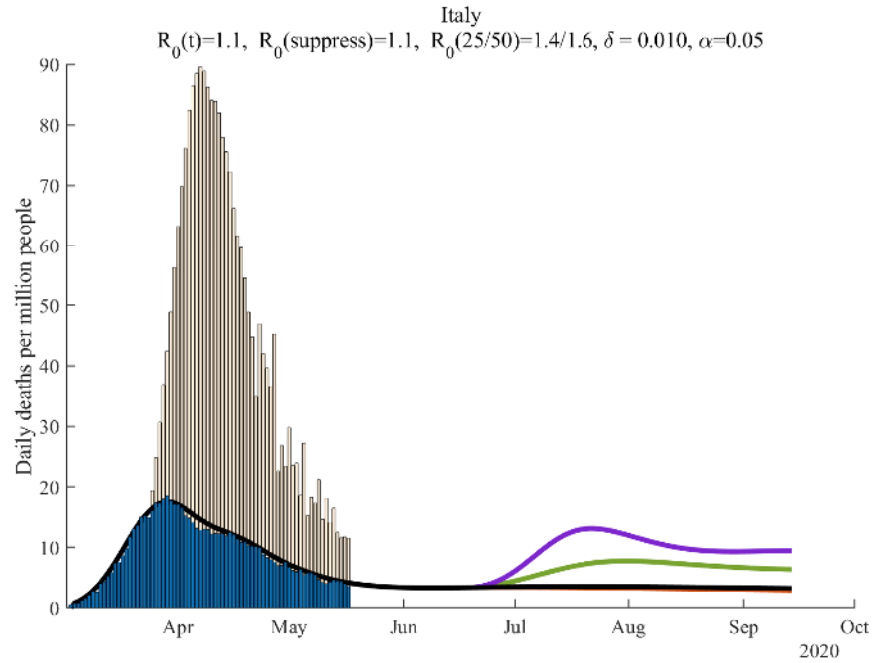
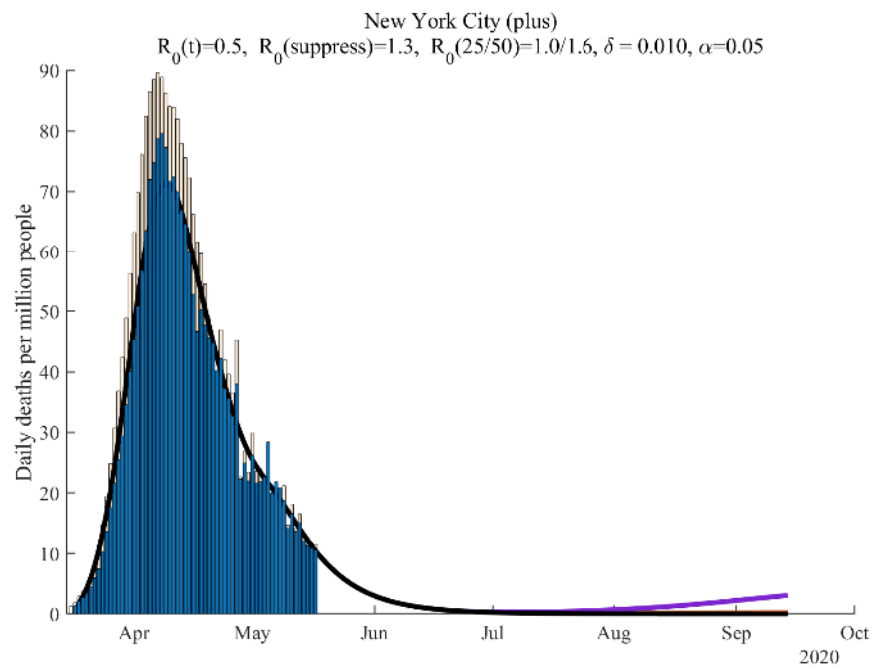
Figure 37: New York City: Re-opening
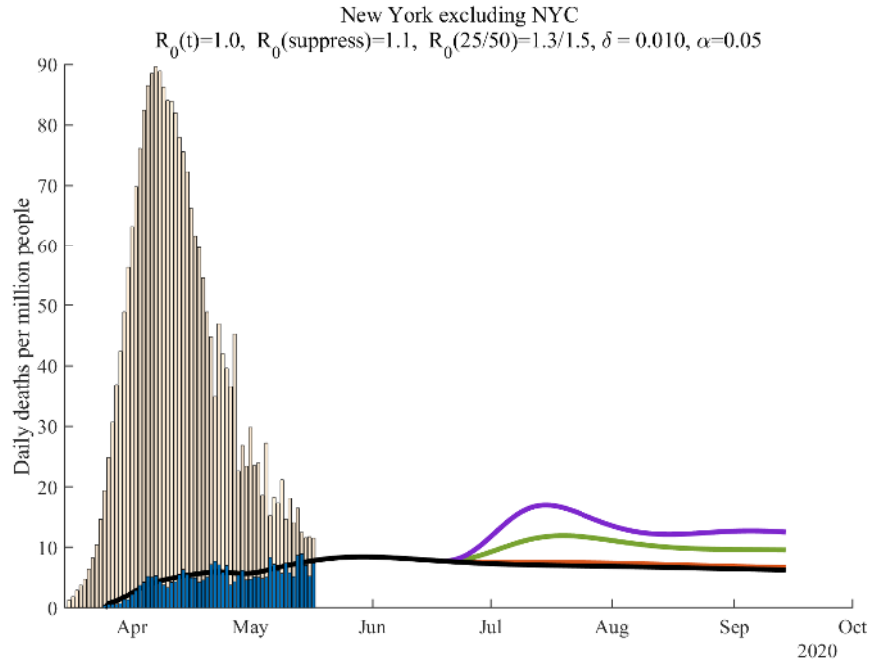
Figure 38: New York excluding NYC: Re-opening

New York excluding NYC
$R_0(t)=1.0$, R_0(suppress)=1.1, $R_0(25/50)=1.3/1.5$, $\delta = 0.010$, $\alpha=0.05$

Figure 39: Los Angeles: Re-opening

Los Angeles
$R_0(t)=1.0$, R_0(suppress)=1.0, $R_0(25/50)=1.2/1.3$, $\delta = 0.010$, $\alpha=0.05$
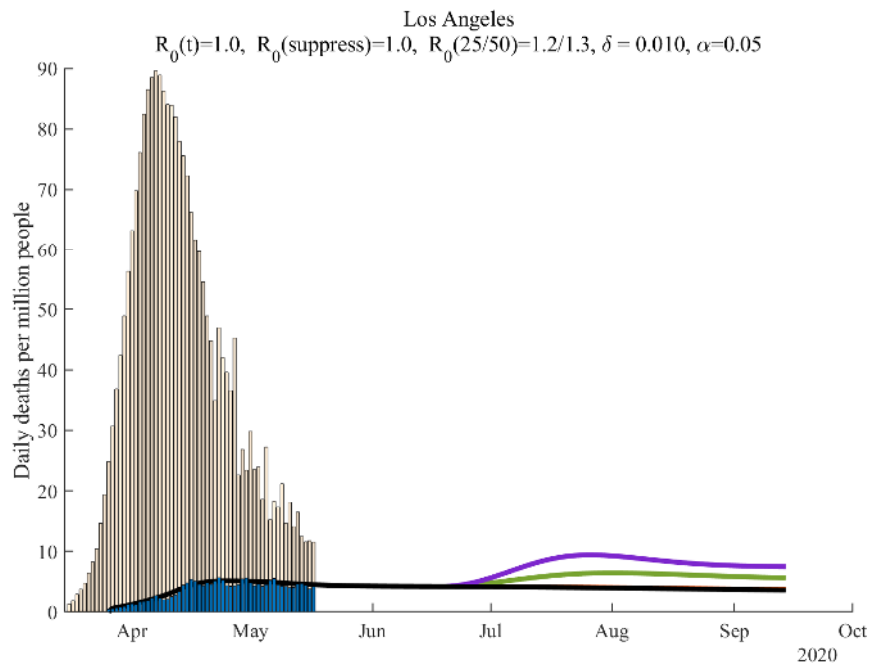
Figure 40: Stockholm, Sweden: Re-opening

Stockholm, Sweden
$R_0(t)=1.5$, $R_0(suppress)=1.3$, $R_0(25/50)=1.8/2.0$, $\delta = 0.010$, $\alpha=0.05$

Figure 41: Chicago: Re-opening

Chicago
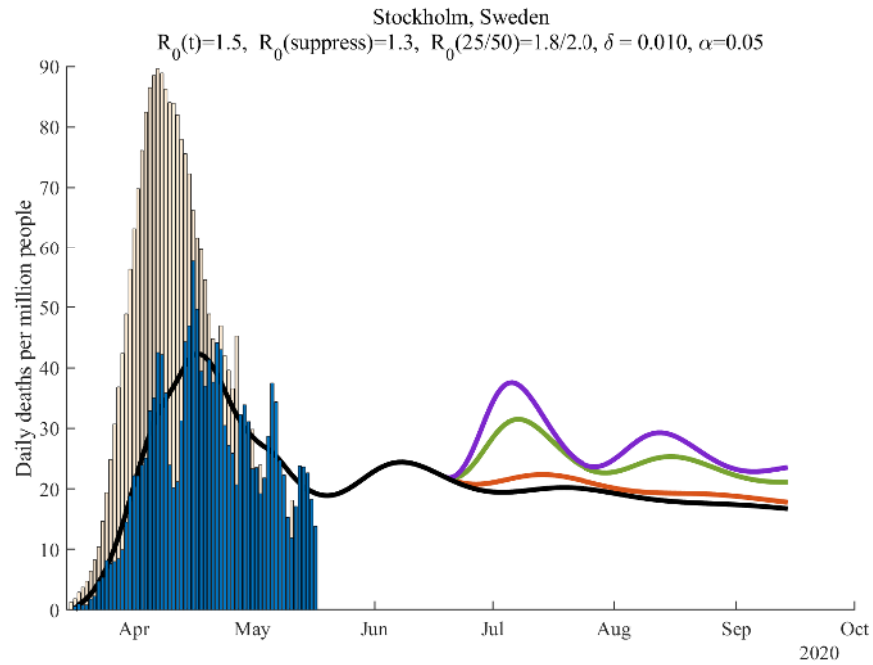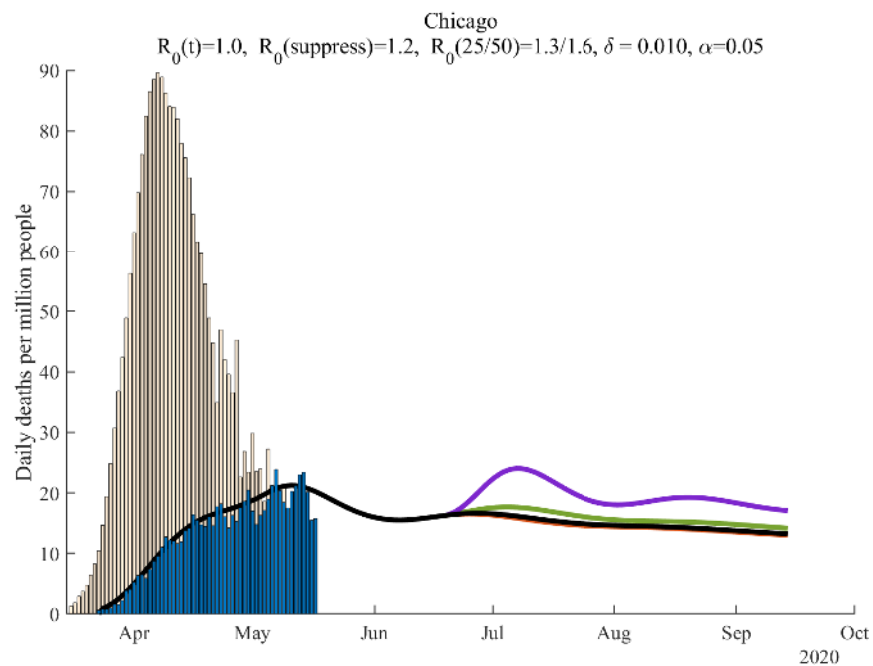$R_0(t)=1.0$, $R_0(suppress)=1.2$, $R_0(25/50)=1.3/1.6$, $\delta = 0.010$, $\alpha=0.05$
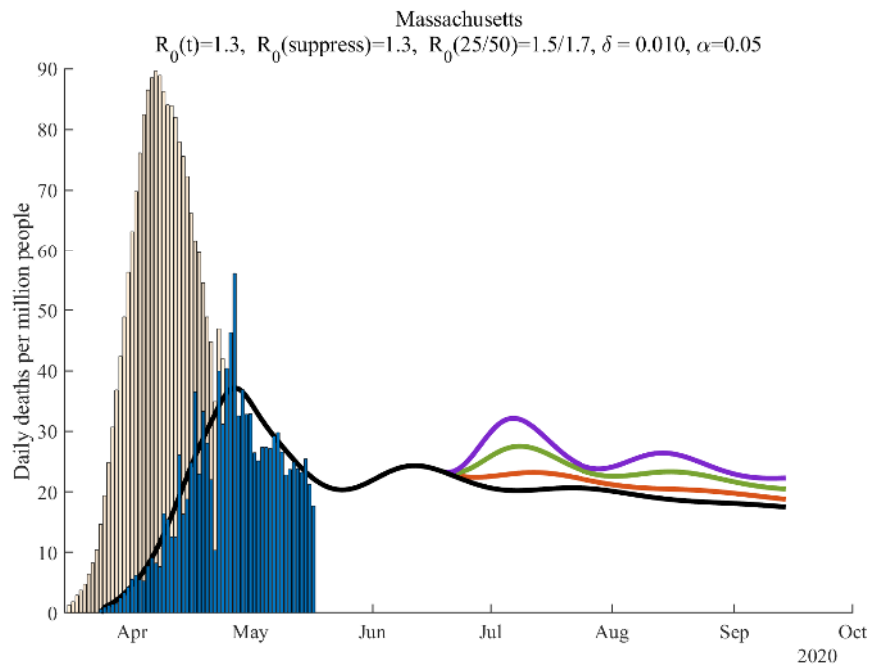
Figure 42: Massachusetts: Re-opening

8.   Conclusions

The first thing to (re)emphasize about these simulations is that we are economists, not epidemiologists. These are speculations based on estimation and simulation of a relatively simple and standard model. We find them helpful for thinking about the dynamics of the pandemic, but great care should be taking in using these numbers to inform any policy discussion.

Relative to the standard SIRD model in the literature, we include a time-varying β, and therefore a time-varying $\mathcal{R}_0$. We invert the SIRD model to back out the daily values of $\mathcal{R}_{0t}$ that fit the death data. We see this as important for capturing behavioral changes by individuals in response to the pandemic as well as policy changes related to social distancing. We also include an additional "recovering" state that is consistent with the medical evidence that cases seem to be infectious for four to five days while taking a total of several weeks or more to resolve. These changes connect the model better to the epidemiology of the virus and are important in improving the model's ability to fit the data. Finally, we follow Cochrane (2020) and include feedback between $\mathcal{R}_{0t}$ and daily deaths in modeling the future of the epidemic. We hope that our empirical estimates will prove useful to others in thinking about the possible path that COVID-19 may take as different locations open up in different ways, and we will continue to update our results on our dashboard.

References

Acemoglu, Daron, Victor Chernozhukov, Iván Werning, and Michael D. Whinston, "A Multi-Risk SIR Model with Optimally Targeted Lockdown," Technical Report, MIT 2020.

Álvarez, Fernando E., David Argente, and Francesco Lippi, "A Simple Planning Problem for COVID-19 Lockdown," Working Paper 26981, National Bureau of Economic Research April 2020.

Atkeson, Andrew, "How Deadly Is COVID-19? Understanding The Difficulties With Estimation Of Its Fatality Rate," Working Paper 26965, National Bureau of Economic Research April 2020.

Avery, Christopher, William Bossert, Adam Clark, Glenn Ellison, and Sara Fisher Ellison, "Policy Implications of Models of the Spread of Coronavirus: Perspectives and Opportunities for Economists," Working Paper 27007, National Bureau of Economic Research April 2020.

Baqaee, David, Emmanuel Farhi, Michael J Mina, and James H Stock, "Reopening Scenarios," Working Paper 27244, National Bureau of Economic Research May 2020.

Bar-On, Yinon M., Avi Flamholz, Rob Phillips, and Ron Milo, "SARS-CoV-2 (COVID-19) by the numbers," Technical Report March 2020.

Bendavid, Eran, Bianca Mulaney, Neeraj Sood, Soleil Shah, Emilia Ling, Rebecca Bromley-Dulfano, Cara Lai, Zoe Weissberg, Rodrigo Saavedra, James Tedrow, Dona Tversky, Andrew Bogan, Thomas Kupiec, Daniel Eichner, Ribhav Gupta, John Ioannidis, and Jay Bhattacharya, "COVID-19 Antibody Seroprevalence in Santa Clara County, California," *medRxiv*, 2020.

Berger, David W, Kyle F Herkenhoff, and Simon Mongey, "An SEIR Infectious Disease Model with Testing and Conditional Quarantine," Working Paper 26901, National Bureau of Economic Research March 2020.

Bethune, Zachary A and Anton Korinek, "Covid-19 Infection Externalities: Trading Off Lives vs. Livelihoods," Technical Report, National Bureau of Economic Research 2020.

Bodenstein, Martin, Giancarlo Corsetti, and Luca Guerrieri, "Social Distancing and Supply Disruptions in a Pandemic," Technical Report 2020-031 04 2020.

Brauer, F., C. Castillo-Chavez, and Z. Feng, *Mathematical Models in Epidemiology*, Springer New York, 2019.

Chari, Varadarajan V, Rishabh Kirpalani, and Christopher Phelan, "The Hammer and the Scalpel: On the Economics of Indiscriminate versus Targeted Isolation Policies during Pandemics," Working Paper 27232, National Bureau of Economic Research May 2020.

Chowell, Gerardo, Cécile Viboud, Lone Simonsen, and Seyed M. Moghadas, "Characterizing the Reproduction Number of Epidemics with Early Subexponential Growth Dynamics," *Journal of The Royal Society Interface*, 2016, *13* (123), 20160659.

Cochrane, John, "An SIR Model with Behavior," May 2020. The Grumpy Economist blog, https://johnhcochrane.blogspot.com/.

Eichenbaum, Martin S, Sergio Rebelo, and Mathias Trabandt, "The Macroeconomics of Epidemics," Working Paper 26882, National Bureau of Economic Research March 2020.

Farboodi, Maryam, Gregor Jarosch, and Robert Shimer, "Internal and External Effects of Social Distancing in a Pandemic," Technical Report 2020-47 2020. University of Chicago, Becker Friedman Institute for Economics Working Paper.

Garriga, Carlos, Rody Manuelli, and Siddhartha Sanghi, "Optimal Management of an Epidemic: An Application to COVID-19. A Progress Report," Technical Report April 2020. Federal Reserve Bank of St. Louis manuscript.

Hethcote, Herbert W., "The Mathematics of Infectious Diseases," *SIAM Review*, 2000, *42* (4), 599–653.

Hornstein, Andreas, "Social Distancing, Quarantine, Contact Tracing, and Testing: Implications of an Augmented SEIR-Mode," Technical Report, Federal Reserve Bank of Richmond 2020.

Hortasu, Ali, Jiarui Liu, and Timothy Schwieg, "Estimating the Fraction of Unreported Infections in Epidemics with a Known Epicenter: an Application to COVID-19," Working Paper 27028, National Bureau of Economic Research April 2020.

Hurwicz, Leonid, "On the Structural Form of Interdependent Systems," in Ernest Nagel, Patrick Suppes, and Alfred Tarski, eds., *Logic, Methodology and Philosophy of Science*, Vol. 44 of *Studies in Logic and the Foundations of Mathematics*, Elsevier, 1962, pp. 232 – 239.

Imperial College COVID-19 Response Team, "Impact of non-pharmaceutical interventions (NPIs) to reduce COVID19 mortality and healthcare demand," Technical Report, Imperial College 2020.

Johns Hopkins University CSSE, "2019 Novel Coronavirus COVID-19 (2019-nCoV) Data Repository," 2020. Center for Systems Science and Engineering.

Karin, Omer, Yinon M Bar-On, Tomer Milo, Itay Katzir, Avi Mayo, Yael Korem, Boaz Dudovich, Eran Yashiv, Amos J Zehavi, Nadav Davidovich et al., "Adaptive cyclic exit strategies from lockdown to suppress COVID-19 and allow economic activity," *medRxiv*, 2020.

Katz, Josh and Margot Sanger-Katz, "N.Y.C. Deaths Reach 6 Times the Normal Level, Far More Than Coronavirus Count Suggests," *The New York Times*, April 2020.

Kermack, William Ogilvy and A. G. McKendrick, "A contribution to the mathematical theory of epidemics, part I," *Proceedings of the Royal Society of London. Series A*, 1927, *115* (772), 700–721.

___ and ___ , "Contributions to the mathematical theory of epidemics. II – The problem of endemicity," *Proceedings of the Royal Society of London. Series A*, 1932, *138* (834), 55–83.

Korolev, Ivan, "Identification and Estimation of the SEIRD Epidemic Model for COVID-19," Technical Report, Binghamton University 2020.

___ , "What Does the Case Fatality Ratio Really Measure?," Technical Report, Binghamton University 2020.

Kucinskas, Simas, "Tracking R of COVID-19," *Available at SSRN 3581633*, 2020.

Linton, Oliver, "When will the Covid-19 pandemic peak?," Technical Report, University of Cambridge 2020.

Liu, Laura, Hyungsik Roger Moon, and Frank Schorfheide, "Panel Forecasts of Country-Level Covid-19 Infections," Working Paper 27248, National Bureau of Economic Research May 2020.

Morton, R. and K. H. Wickwire, "On the Optimal Control of a Deterministic Epidemic," *Advances in Applied Probability*, 1974, *6* (4), 622–635.

New York Department of Health, "The NYSDOH Wadsworth Center's Assay for SARS-CoV-2 IgG," Technical Report April 2020.

Sanche, S., Y.T. Lin, C. Xu, E. Romero-Severson, N. Hengartner, and R. Ke, "High contagiousness and rapid spread of severe acute respiratory syndrome coronavirus 2," *Emerging Infectious Diseases*, 2020, *26*.

Stock, James H, "Data Gaps and the Policy Response to the Novel Coronavirus," Working Paper 26902, National Bureau of Economic Research March 2020.

The Economist, "Tracking covid-19 excess deaths across countries," April 2020.

Toda, Alexis Akira, "Susceptible-Infected-Recovered (SIR) Dynamics of COVID-19 and Economic Impact," 2020. U.C.S.D. manuscript.

A.   Graphs for Other Countries, States, and Cities

Graphs for many countries and regions are shown below. We report detailed and extended results for even more countries, states, and cities on our web pages and plan to update the dashboard frequently.

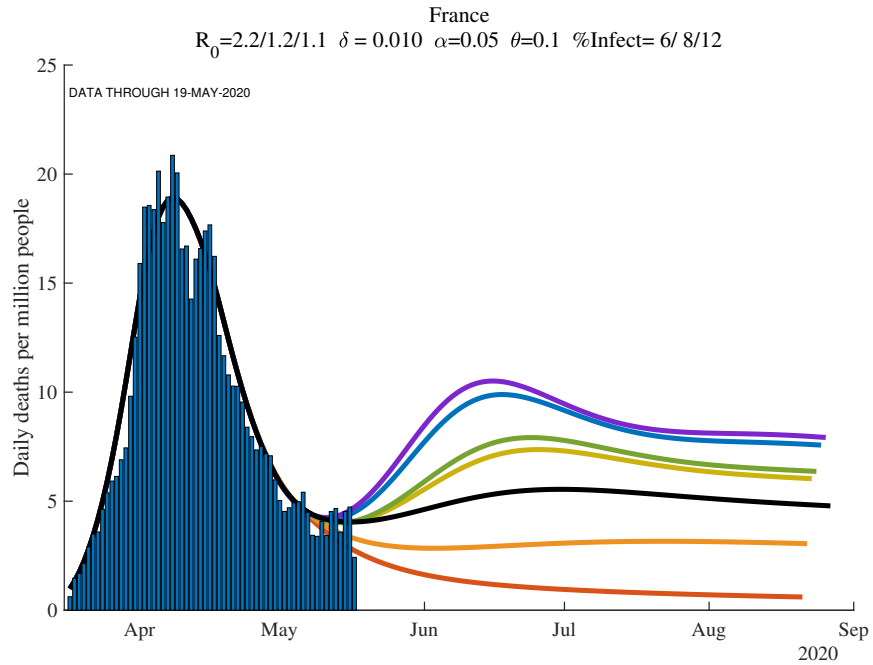Figure 43: France (7 days): Daily Deaths per Million People

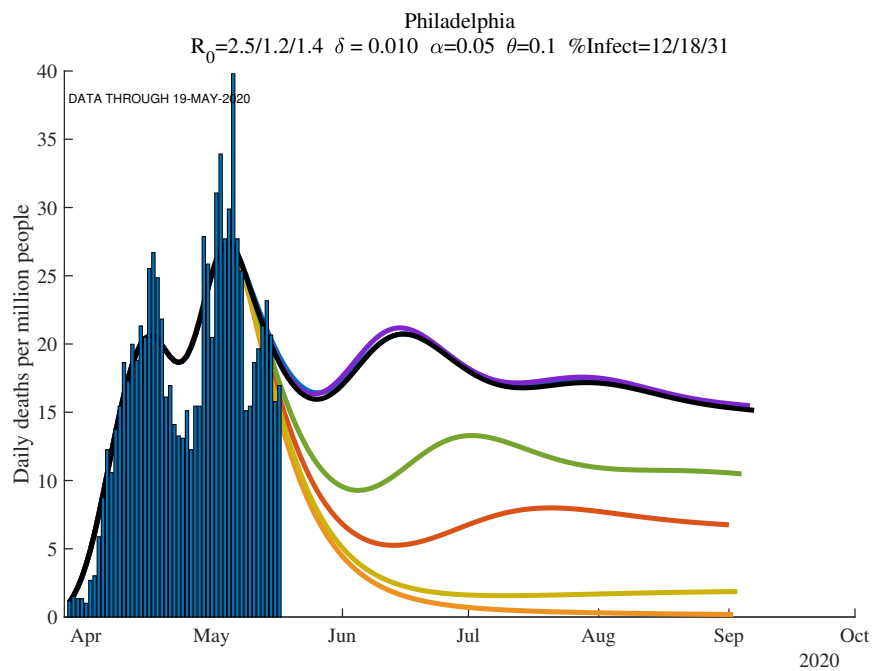Figure 44: Philadelphia (7 days): Daily Deaths per Million People

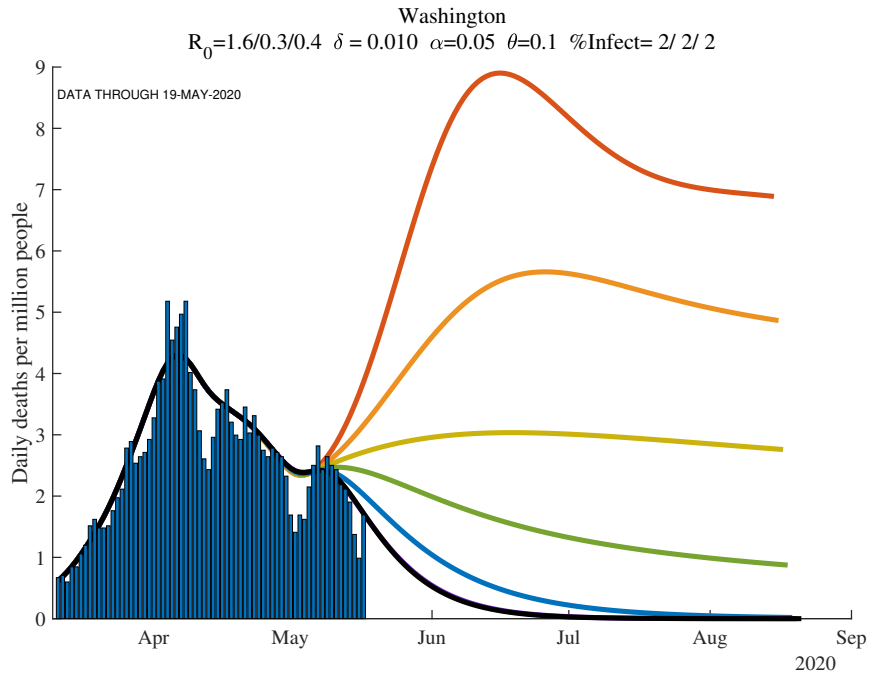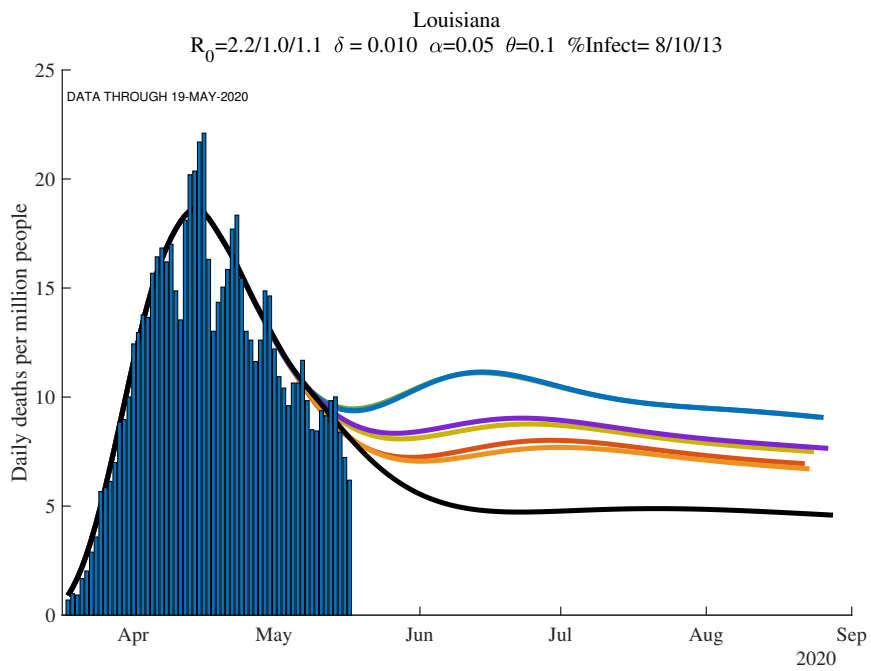## Figure 45: Washington (7 days): Daily Deaths per Million People

Washington
R_0=1.6/0.3/0.4 δ = 0.010 α=0.05 θ=0.1 %Infect= 2/ 2/ 2

DATA THROUGH 19-MAY-2020

Figure 46: Louisiana (7 days): Daily Deaths per Million People

Louisiana
R_0=2.2/1.0/1.1 δ = 0.010 α=0.05 θ=0.1 %Infect= 8/10/13

DATA THROUGH 19-MAY-2020

Figure 47: Florida (7 days): Daily Deaths per Million People

Florida
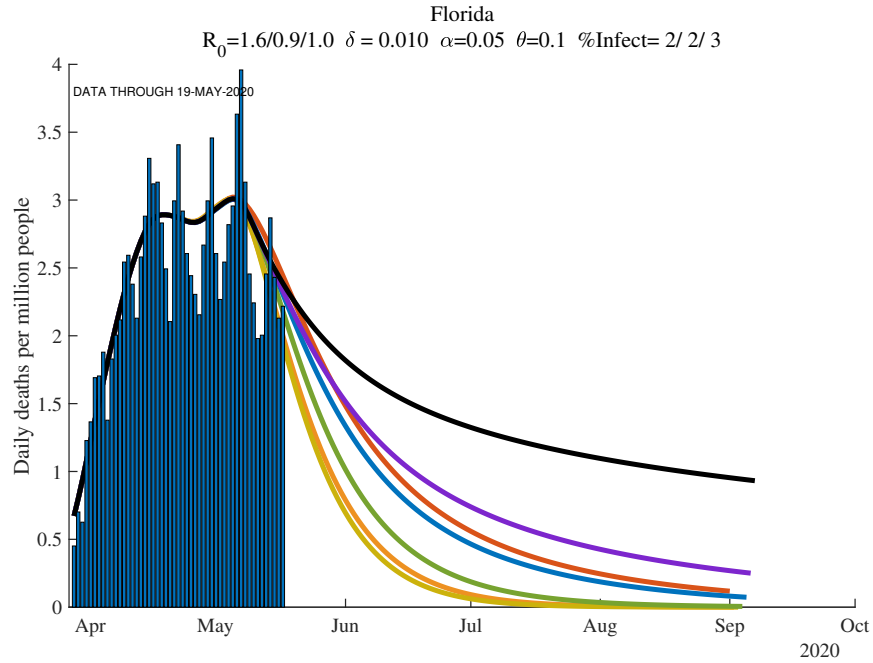R_0=1.6/0.9/1.0 δ = 0.010 α=0.05 θ=0.1 %Infect= 2/ 2/ 3

DATA THROUGH 19-MAY-2020

Figure 48: Connecticut (7 days): Daily Deaths per Million People

Connecticut
R_0=2.5/1.5/1.7 δ = 0.010 α=0.05 θ=0.1 %Infect=17/25/43

DATA THROUGH 19-MAY-2020